INFORMATION TO USERS

This manuscript has been reproduced from the microfilm master. UMI films the text directly from the original or copy submitted. Thus, some thesis and dissertation copies are in typewriter face, while others may be from any type of computer printer.

The quality of this reproduction is dependent upon the quality of the copy submitted. Broken or indistinct print, colored or poor quality illustrations and photographs, print bleedthrough, substandard margins, and improper alignment can adversely affect reproduction.

In the unlikely event that the author did not send UMI a complete manuscript and there are missing pages, these will be noted. Also, if unauthorized copyright material had to be removed, a note will indicate the deletion.

Oversize materials (e.g., maps, drawings, charts) are reproduced by sectioning the original, beginning at the upper left-hand corner and continuing from left to right in equal sections with small overlaps.

Photographs included in the original manuscript have been reproduced xerographically in this copy. Higher quality 6" x 9" black and white photographic prints are available for any photographs or illustrations appearing in this copy for an additional charge. Contact UMI directly to order.

Bell & Howell Information and Learning
300 North Zeeb Road, Ann Arbor, MI 48106-1346 USA
800-521-0600

UMI®

Université d'Ottawa • University of Ottawa

Short-term Recovery from a Volume Increase in the Mouse Zygote: Characteristics of Regulatory Volume Decrease In Vitro

© Diane G Séguin

Thesis submitted to the Faculty of Graduate and Postdoctoral Studies as a partial fulfilment of the M.Sc. program in the Cellular and Molecular Medicine Graduate Program, Faculty of Medicine, University of Ottawa
December 1999 ©

Supervisor: Jay M Baltz
Loeb Health Research Institute
Ottawa Hospital, Civic Campus
Ottawa, Ontario
Canada

ABSTRACT

Mouse zygotes have been shown to recover from an imposed increase in volume, a process known as a regulatory volume decrease or RVD, via separate but functionally coupled Cl^- and K^+ channels. The objectives of this thesis were to further determine some of the characteristics of these Cl^- and K^+ channels involved in RVD in the mouse zygote. Results show that intracellular Ca^{++} concentration increased upon cell swelling in mouse zygotes; however, RVD occurred normally in zygotes loaded with the Ca^{++} chelator, BAPTA. In addition, known inhibitors of Ca^{++}-dependent K^+ channels, charybdotoxin and apamin, had no effect on RVD. Results also demonstrate that mouse zygote RVD was inhibited by 5 mM extracellular ATP but was insensitive to millimolar levels of adenosine or cAMP. It was proposed that the Cl^- channel in mouse zygotes was a swelling-activated Cl^-/organic osmolyte channel like that found in many other cells. A method developed by Passantes-Morales et al. (1993) was used, in which a large extracellular concentration of one of a number of organic osmolytes was added to the experimental media, and the ability of the zygote to perform RVD in the presence of each was determined. A number of organic compounds demonstrated an inhibition of RVD, and thus, identified a number of organic compounds which might function as organic osmolytes in embryos. To directly test whether swelling of zygotes increased their permeability to organic osmolytes; the permeability in swelled zygotes was compared to

that in non-swelled zygotes, using ^{3}H glycine. ^{3}H-glycine concentrations were significantly higher in zygotes exposed to hypotonic conditions versus isotonic conditions. Glycine permeability, in hypotonic conditions, was inhibited in the presence of DIDS and ATP, which are known blockers of the swelling-activated Cl^- and organic osmolyte channel in the mouse zygote and other cells.

From the results presented here, it is concluded that Ca^{++} -sensitive K^+ channels are not required in RVD. The effects of ATP, adenosine, cAMP are consistent with the characteristics of the swelling-activate Cl^- channels which are also permeable to organic osmolytes; it is therefore suggested that this channel plays an important role in the process of RVD in the mouse zygote.

ACKNOWLEDGEMENTS

I would like to thank my supervisor, Dr. J. M. Baltz, for providing me with guidance, Ms. K. Dawson for excellent technical assistance, and Dr. K. Burns, Dr. P. Doroshenko, and Dr. W. Gibb for very helpful discussions.

I would like to thank the Department of Ob/Gyn, Ottawa Hospital, Civic Campus and the Division of Reproductive Medicine, Department of Ob/Gyn, University of Ottawa for my Graduate Studentship.

I would like to express my gratitude to my parents, J. and T. Séguin, and to my husband, M. Allan, for their continuous support and encouragement.

The Medical Research Council of Canada (MRC) Operating Grant MT12040 supported this work.

TABLE OF CONTENTS

LIST OF ABBREVIATIONS

A9C	antracene-9-carboxylic acid
ADP	adenosine 5'-diphosphate
AMP	adenosine 5'-monophosphate
ANOVA	analysis of variance
ATP	adenosine 5'-triphosphate
BSA	bovine serum albumin
Ca^{++}	calcium ion
CAMP	adenosine3':5'-cyclic monophosphate
Cl^{-}	chloride ion
Con	control
CTX	charybdotoxin
DAG	1-2 diacylglycerol
DIDS	4,4'-diisothiocyanatostilbene-2,2'-disulfonic acid
DMSO	dimethylsulfoxide
DPC	diphenylamine carboxylate
EGTA	ethylene glycol-bis [ß-aminoethyl ether]-N,N,N',N'-tetraacetic acid
FSH	follicle-stimulating hormone
HCG	human chorionic gonadotropin
Hepes	N-2-hydroxyethylpiperazine-N'2-ethanesulfonic acid
IAA-94	Indanyl-oxyacetic acid
IU	international units
K^{+}	potassium ion
KSOM	K^{+}-supplemented simplex optimized media
LH	luteinizing hormone
MDCK	Madin-Darby canine kidney
mOsm	milliOsmolar
NPPB	5-nitro-2-(3-phenylpropylamino)benzoic acid
PKC	protein kinase C
PMSG	pregnant mare serum gonadotropin
PVA	polyvinyl alcohol
RVD	regulatory volume decrease
RVI	regulatory volume increase
SEM	standard error of the mean
VSOAC	volume-sensitive organic osmolyte/anion channel
VSOR	volume-sensing outwardly rectifying

LIST OF TABLES

LIST OF FIGURES

INTRODUCTION

1. Embryo Development

Gametogenesis

The genetic basis of reproduction and sex determination relies on the formation of haploid gametes by meiosis, via two successive cell divisions, called the first and second meiotic divisions. At the completion of meiosis, each of the four resulting gametes has one representative of each of the homologous pairs of autosomal chromosomes, and one of the sex chromosomes. Combination of the nuclei of two gametes in fertilization restores the diploid complement of chromosomes in the fertilized ovum (a zygote).

On the chromosomal level, the events of meiosis are similar in the ovary and testis (Figure 1). However, the timing of meiosis and the acquisition of specialized features after the completion of meiosis are notably different between sperm and oocyte. The male gamete proceeds directly from continuous mitotic divisions of the stem cell population, the spermatogonia, to continuous meiotic divisions. The resulting haploid male reproductive cell subsequently undergoes a process called spermiogenesis or spermiation after the completion of meiosis in which it acquires the specific cellular mechanisms it needs to reach and fertilize the ovum once deposited in the female reproductive tract.

In contrast, the mitotic divisions of the female germ cell are completed very early

in the life of the animal, and the oocyte is arrested at the first prophase before birth and remains arrested until after puberty. It only resumes meiotic division at ovulation. The cytoplasm of the primary oocyte is unevenly distributed during the two meiotic divisions; i.e. unequal cleavages. This process, called oogenesis, produces one functional ovum, which contains most of the original cytoplasm, and two nonfunctional polar bodies that later disintegrate (although a polar body might cleave once before disintegrating). At ovulation, the ovary releases a secondary oocyte rather than a mature ovum, which is suspended in metaphase of meiosis II. The completion of the second meiotic division only occurs when the egg is activated by fertilization (Figure 1).

Figure 1

Gametogenesis

Oogenesis: Schematic diagram of meiosis in the ovary, showing the production of an ovum and two or three nonfunctional polar bodies from a single primary oocyte.

Spermatogenesis: Schematic diagram of meiosis in the testis, showing the distribution of only a few chromosomes.

Adapted from Martini et al. (1998).

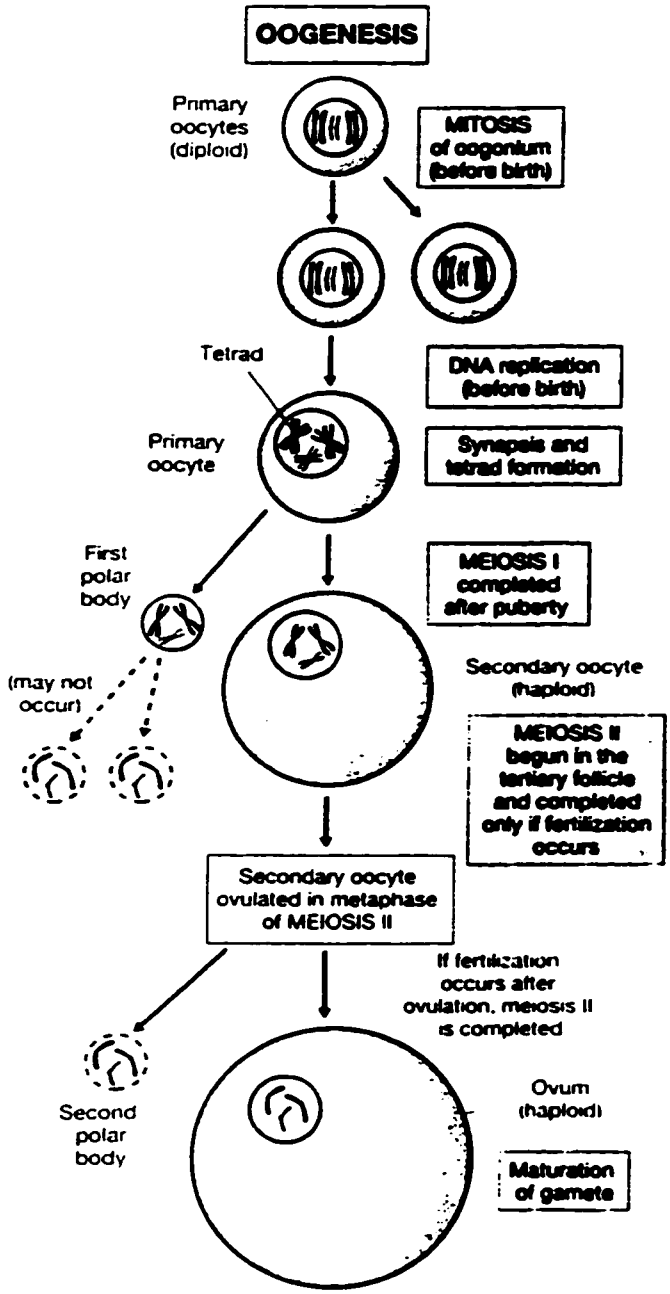
OOGENESIS
Primary oocytes (diploid)
MITOSIS of oogonium (before birth)
Tetrad
DNA replication (before birth)
Primary oocyte
Synapsis and tetrad formation
First polar body
MEIOSIS I completed after puberty
(may not occur)
Secondary oocyte (haploid)
MEIOSIS II begun in the tertiary follicle and completed only if fertilization occurs
Secondary oocyte ovulated in metaphase of MEIOSIS II
If fertilization occurs after ovulation, meiosis II is completed
Second polar body
Ovum (haploid)
Maturation of gamete

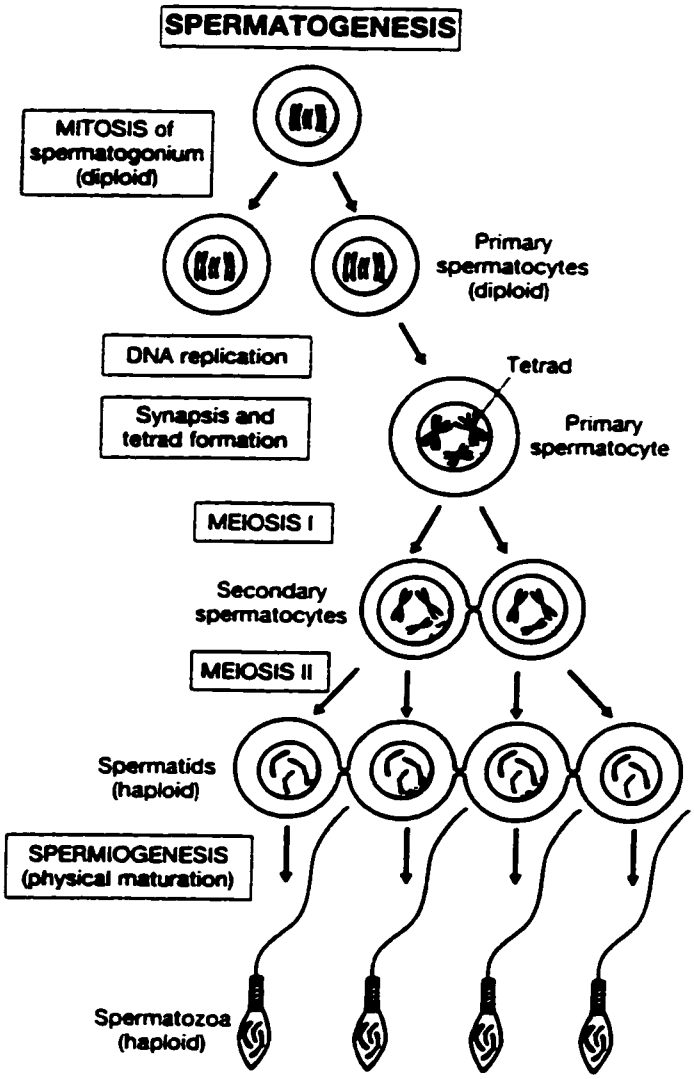
SPERMATOGENESIS
MITOSIS of spermatogonium (diploid)
Primary spermatocytes (diploid)
DNA replication
Synapsis and tetrad formation
Tetrad
Primary spermatocyte
MEIOSIS I
Secondary spermatocytes
MEIOSIS II
Spermatids (haploid)
SPERMIOGENESIS (physical maturation)
Spermatozoa (haploid)

Spermatozoon

A typical sperm cell, a spermatozoon, has three distinct regions: (1) the head, (2) the middle piece, and (3) the tail (Figure 2). The head of the sperm is a flattened ellipse, containing a nucleus which holds the densely packed genetic information, and components of the acrosome, i.e. a membranous compartment containing enzymes essential to the process of fertilization at the anterior tip of the sperm head. The acrosome aids the sperm in penetrating the outer egg coat and establishing connection with the egg membrane. Directly behind the nucleus, in the neck region of the sperm, are the mitochondria and centrioles. The microtubules of the distal centrioles are continuous with those of the middle piece. The mitochondria are arranged in a spiral around the microtubules in the middle piece. Mitochondrial activity provides the ATP that is needed for motility of the tail. The tail, composed of a fibrous sheath of flagellum propels the cell.

Figure 2

Spermiogenesis and spermatozoon structure

Differentiation of a spermatid into a spermatozoon.

Adapted from Martini et al. (1998).

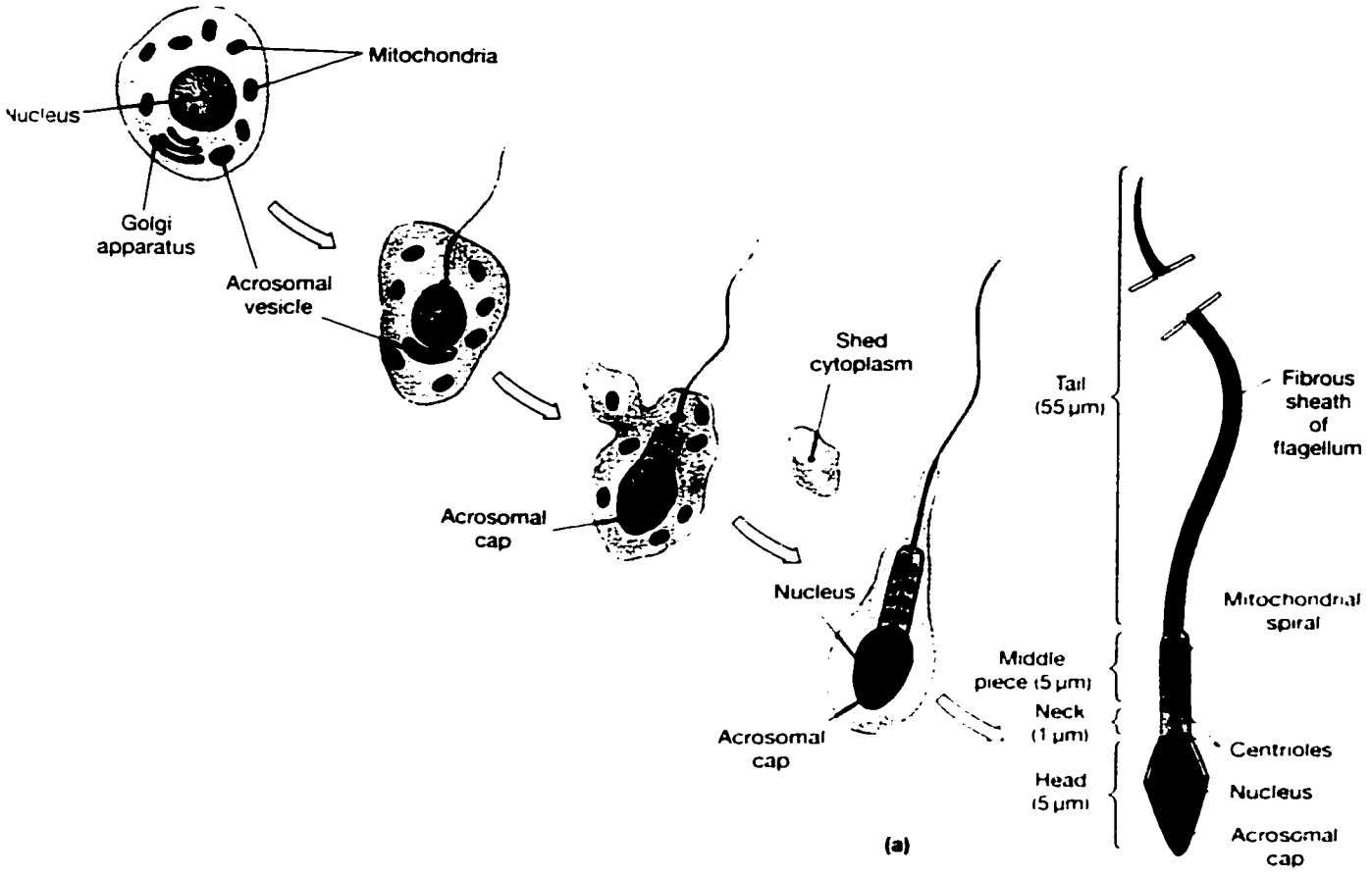
Mitochondria
Nucleus
Golgi apparatus
Acrosomal vesicle
Acrosomal cap
Shed cytoplasm
Nucleus
Acrosomal cap
Tail (55 µm)
Middle piece (5 µm)
Neck (1 µm)
Head (5 µm)
Fibrous sheath of flagellum
Mitochondrial spiral
Centrioles
Nucleus
Acrosomal cap
(a)

Ovum

An ovarian follicle is a specialized structure in which oocyte growth and meiosis I occur. The ovarian cycle can be divided into a follicular phase, or preovulatory phase, and a luteal phase, or postovulatory phase. Follicle formation is stimulated by FSH (follicle-stimulating hormone) from the anterior pituitary. The ovarian cycle begins as activated primordial follicles develop into primary follicles (Figure 3). In a primary follicle, the follicular cells enlarge and undergo repeated cells divisions. The divisions create several layers of follicular cells, called granulosa cells, around the oocyte. As layers of granulosa cells develop around the primary oocyte, microvilli from the surrounding cells intermingle with those of the primary follicle. The microvilli are surrounded by a shell composed of glycoproteins called the zona pellucida. The microvilli increase the surface area available for the transfer of materials from the granulosa cells to the rapidly enlarging oocyte. The transformation of primary follicles to secondary follicles is marked by the thickening of the follicular wall and the secretion of fluid from the granulosa cells. Follicular fluid accumulates in small pockets that gradually expand to form a cavity (antrum) which separates the inner and outer layers of the follicle. Under the influence of FSH, the follicle continues to mature and forms the Graaffian follicle. A surge of LH (luteinizing hormone) causes the Graaffian follicle to ovulate and the remnant of the follicle becomes a corpus luteum, which maintains the

receptivity of the uterus to a pregnancy by secreting estradiol and progesterone. If pregnancy does not occur, the uterine receptive period is terminated and the degeneration of the corpus luteum begins leaving a scarlike corpus albicans.

Figure 3

Life cycle of an ovarian follicle

A single primary oocyte (A) serves as a basis for a primary follicle (B). Several primary follicles advance to the secondary follicle stage (C) over several menstrual cycles. One of several follicles per cycle continues to mature (D) under the influence of FSH and reaches the Graaffian stage (E). A surge of LH causes the Graaffian follicle to ovulate (F). After ovulation, the remnant of the follicle becomes a corpus luteum (G). If pregnancy does not occur, the corpus luteum degenerates leaving a scarlike corpus albicans (H).

Adapted from Schauf et al. (1990).

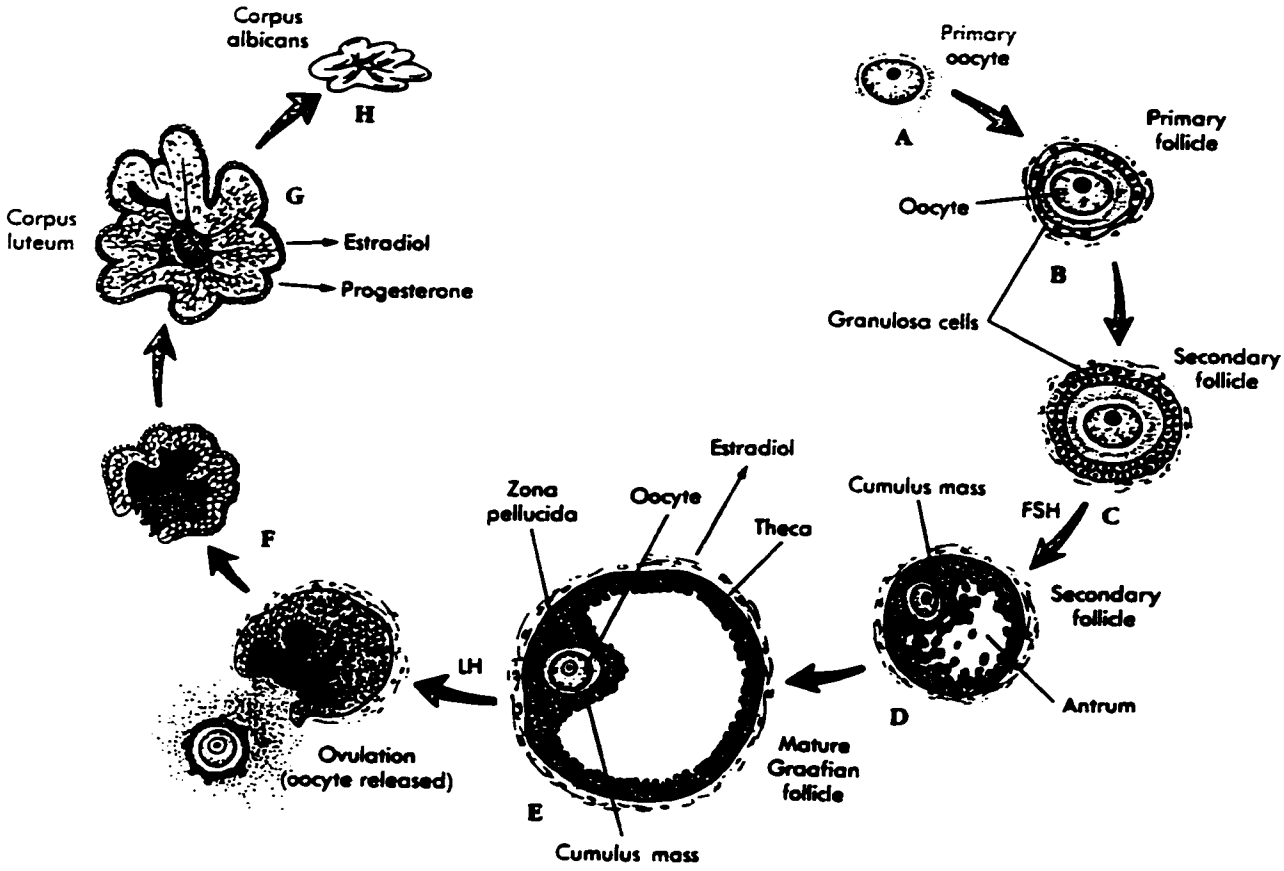
Corpus albicans
H
Corpus luteum
G
Estradiol
Progesterone
F
LH
Ovulation (oocyte released)
Zona pellucida
Oocyte
Estradiol
Theca
Cumulus mass
E
Mature Graafian follicle
D
Antrum
Cumulus mass
FSH
C
Secondary follicle
Granulosa cells
B
Primary follicle
Oocyte
A
Primary oocyte

Fertilization

Fertilization is the process by which male and female gametes fuse in the ampullary region of the oviduct usually called the Fallopian tube in humans. Once they enter the female reproductive tract, spermatozoa move rapidly from the vagina into the uterus and subsequently into the oviducts. The sperm moves through the hyaluronic acid matrix between cumulus cells, a process which requires both motility and the action of hyaluronidase secreted by the sperm. The sperm then contacts the zona pellucida. Specific binding of receptors on the sperm surface, whose identity is as yet unknown, to the glycoprotein components of the zona pellucida results in both adhesion of the sperm to the zona pellucida, and the triggering of the exocytosis of the acrosome. This acrosome reaction releases enzymes which allow the sperm to penetrate the zona pellucida. At contact with the oocyte membrane, another set of receptor-ligand biding events mediate the fusion of the sperm and egg plasma membranes. Fusion activates the oocyte to complete its meiotic division to form a distinct female pronucleus (genetic material of the oocyte). Activation is mediated by a transient increase in intracellular Ca^{++}. After entering the egg cytoplasm, the sperm nucleus decondenses and forms the male pronucleus. Both the male pronucleus and female pronucleus migrate towards the centre of the egg. The two pronuclei finally fuse in a process called syngamy. In some animals (e.g., mice) fusion of the pronuclei occurs coincident with the first cell division.

The fertilized egg is called the zygote, which is the subject of the studies reported here.

Cleavage

Approximately 24 hours after fertilization, the zygote undergoes the first cleavage division, developing into subsequent embryo stages via a series of reductive cleavages that subdivide the cytoplasm of the zygote within the extracellular matrix shell-the zona pellucida (Figure 4). The increase in cell number occurs without the intervening growth between successive cell divisions. Thus, blastomere volume is decreased during cleavage to produce smaller cells that participate in the subsequent morphogenic events that mold the embryo. Just prior to entering the uterus, the embryo, now in its 16-cell stage (in mice), undergoes a process known as compaction, wherein the cells become tightly associated via cell adhesion molecules and gap junctions, forming the morula. In the uterus, the outer cells of the morula differentiate into a fluid transporting epithelium, which forms a fluid-filled cavity (blastocoele). The subsequent cavitating embryo forms the blastocyst, which consists of three compartments: the enclosing epithelium (trophoblast), the fluid-filled blastocoele cavity, and the inner cell mass, which adheres to the inner surface at one pole of the trophoblast within the blastocoele (Figure 4). The inner cell mass is fated to form the embryonic tissues and some extraembryonic tissues, whereas the trophoblast is the precursor of part of the placenta and is the earliest

component of the system of extraembryonic structures. Once the zona pellucida has been shed, the cells of the trophoblast come in close contact with the wall of the uterus, in which the embryo becomes implanted. Meanwhile the inner cell mass grows and part of it begins to differentiate, forming first of all two further extraembryonic structures: the amniotic sac and the yolk sac. Once these structures have developed, the rest of the inner cell mass goes on to form the embryo proper by further processes of growth and differentiation.

Figure 4

Cleavage and blastocyst formation

Adapted from Martini et al. (1998).

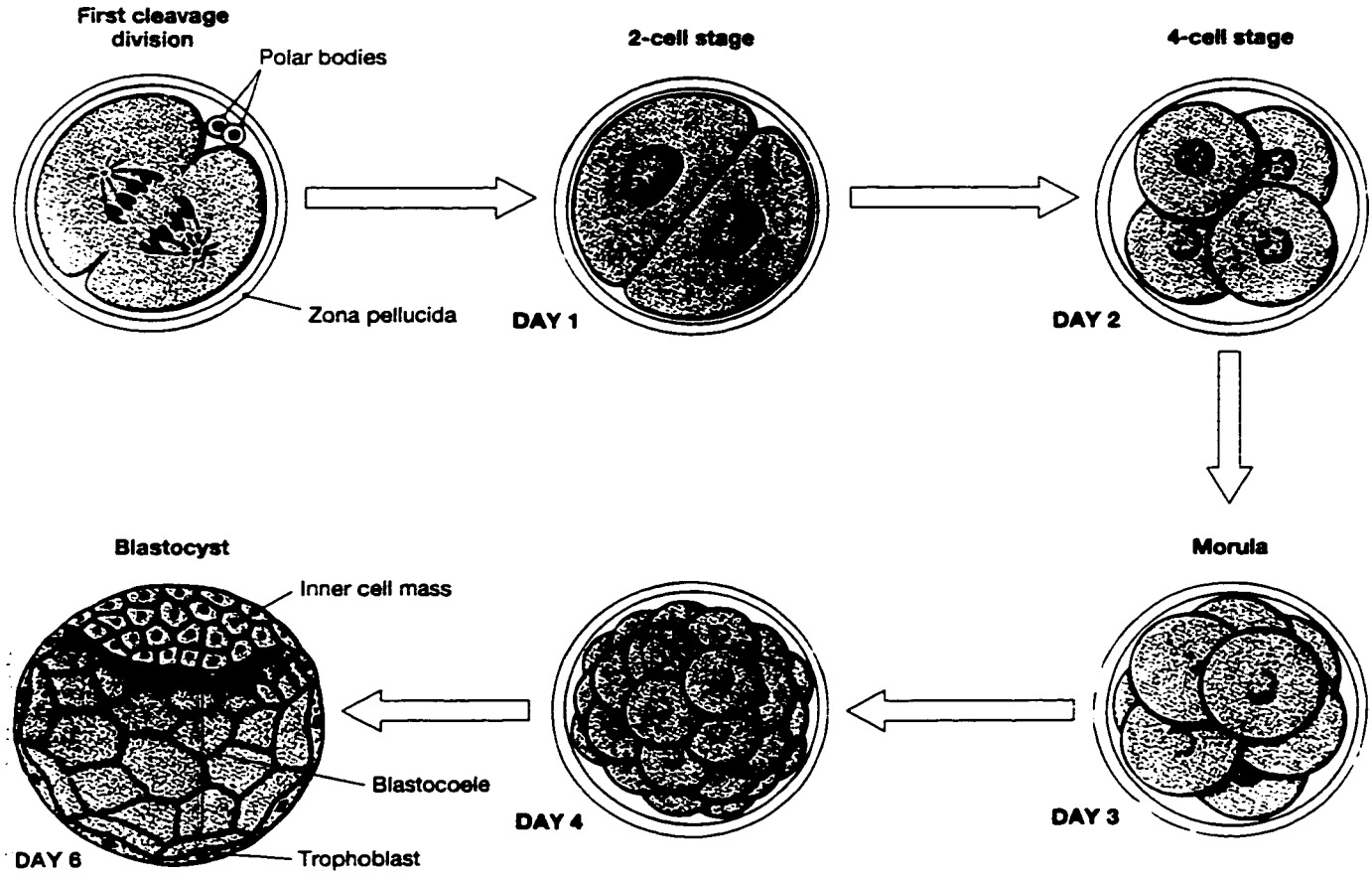
First cleavage division
Polar bodies
Zona pellucida
DAY 1
2-cell stage
DAY 2
4-cell stage
Morula
DAY 3
DAY 4
Blastocyst
Inner cell mass
Blastocoele
Trophoblast
DAY 6

Development and Embryo Environment

A preimplantation mammalian embryo, particularly the zygote, can be adversely affected by its environment. Any changes within the embryo's surroundings such as fluctuations in osmolarity and solute concentrations can be detrimental to its development, and mammalian embryos have been reported to be particularly susceptible to changes in osmolarity (Biggers et al., 1993; Borland et al., 1977; Davidson et al., 1988; Dawson and Baltz, 1997; Spindle, 1995; Van Winkle et al., 1990).

Preimplantation mammalian embryos have been shown to be very sensitive to increased external osmolarity: most zygotes fail to develop in vitro at osmolarities above 300 mOsm (Biggers et al., 1993; Davidson et al., 1988; Dawson and Baltz, 1997; Hay-Schmidt, 1993). This was not easy to reconcile with calculations, based on electron probe X-ray microanalysis data, which indicated that the osmolarity of oviductal fluid was greater than 340 mOsm (Borland et al., 1977; Van Winkle et al., 1990). However, more recent measurements which used embryos themselves as osmometers to determine the tonicity of mouse oviductal fluid indicated instead that the osmolarity was about 300 mOsm (Collins and Baltz, 1999).

In vitro embryo development is identically inhibited by raised osmolarity whether produced by added NaCl or raffinose, demonstrating that high osmolarity is itself detrimental to embryos (Dawson and Baltz, 1997). However, development can occur at

higher osmolarities if any of a number of organic compounds are present within the medium (Biggers et al., 1993; Dawson and Baltz, 1997; Van Winkle et al., 1990). The presence of betaine (Anbari and Schultz, 1993; Biggers et al., 1993), glycine (Dawson and Baltz, 1997), or taurine (Van Winkle et al., 1990) within the culture medium has been shown to alleviate the detrimental effects of high osmolarity on embryo development in preimplantation mouse conceptuses. Dawson and Baltz (1997) demonstrated that preimplantation embryos are capable of accumulating the organic compound glycine via the Gly system to replace inorganic ions within the embryo's cytoplasm, thus providing intracellular osmotic support when osmolarity is increased. Similarly, Van Winkle et al. (1990) showed the osmotic regulation of taurine transport via system β with taurine transport being stimulated by increased osmolarity.

The use of such mechanisms allows the accumulation of "organic osmolytes" which are necessary for cell viability and normal metabolism when external osmolarity is increased. High intracellular ionic strength has been found to disrupt metabolism and biochemical processes in cells (Yancey, 1994; Yancey et al., 1982). Thus, an increased concentration of inorganic ions would be detrimental. To alleviate this problem, many organisms have evolved mechanisms which allow the accumulation of uncharged organic compounds, or "compatible organic osmolytes," instead of charged inorganic ions. Thus, uncharged organic molecules replace inorganic ions to provide a portion of osmotic

support, allowing total intracellular ion concentration or ionic strength to be held constant while still providing control over intracellular osmolarity (Yancey, 1994; Yancey et al., 1982).

Increased external salt concentration, particularly NaCl, and increased osmolarity inhibits in vitro development to blastocysts (Biggers et al., 1993; Hay-Shmidt, 1993; Van Winkle et al., 1990) and is sufficient to produce a 2-cell block in sensitive mice strains such as inbred and random-bred mice, and in rats, wherein zygotes do not develop past the 2-cell cleavage stage in culture (Biggers et al., 1993; Lawitts and Biggers, 1993; Miyoshi et al., 1994). In the absence of organic osmolytes, the 2-cell block strains can be prevented if the NaCl concentration and thus osmolarity of the culture media is reduced (Biggers et al., 1993; Chatot et al., 1989; Lawitts and Biggers, 1993; Lawitts and Biggers, 1991). Recently, media (e.g., KSOM and CZB) have been developed which overcome the 2-cell block (Chatot et al., 1989; Erbach et al., 1994; Lawitts and Biggers, 1993; Lawitts and Biggers, 1991). One thing these media have in common is their low osmolarity (250-275 mOsm). Another feature of these media is the inclusion of compounds (principally glutamine) which can function as organic osmolytes (Chatot et al., 1989; Dawson and Baltz, 1997; Lawitts and Biggers, 1993). The success of these media indicated a crucial role of osmolarity in permitting embryo development in vitro, and pointed towards a role for organic osmolytes in embryo physiology.

Little was known about the regulation of volume or intracellular osmolarity in embryos. It was clear that low osmolarity was beneficial, and that organic osmolytes allowed development at higher osmolarities, but none of the physiological mechanisms had been identified. It could be inferred, however, that embryos needed both mechanisms for the regulated accumulation of organic osmolytes, and for their regulated release.

Clinical Relevance

There exist many factors that contribute to infertility in the human population. Some factors are treatable, yet most still remain irreversible. It is therefore not surprising to see more patients depending on the intervention of In Vitro Fertilization (IVF) and related techniques to enhance their chance of conception. However, human IVF still remains a developing technology and will require technical improvements to increase its success rate. One area which requires substantial improvement is the ability to grow healthy embryos in vitro. For this, optimal culture media must be developed. Such optimal culture media can only be formulated if the physiological requirements of early embryos are known, including which organic osmolytes are required, and how to support normal cell volume regulation by the embryo.

Determining the characteristics and mechanisms of volume regulation in the preimplantation embryo might reveal particular compounds that are required by the

developing embryo. Hence, knowing the functional actions of particular volume regulatory mechanisms might facilitate the improvement of preimplantation embryo culture media in clinical human IVF laboratories. Understanding the volume regulatory systems will, in addition, enable a better understanding of the role of culture osmolarity and composition in the pathophysiology and morbidity of preimplantation embryos.

2. Volume Regulation

Control of Cell Volume

It has been long recognized that in animal cells, which lack rigid cell membranes and thus cannot support substantial pressure gradients, the control of cell volume is achieved through the regulation of intracellular solute content. Volume regulation is achieved by controlling osmolarity. Osmolarity is defined as the solute content of a solvent (in the case of cells, water), as the molar concentration of total osmotically active species per unit volume. In contrast, osmolality is defined as the moles of osmotically active solute per unit mass, and is the quantity actually measured by osmometers. However, for dilute solutions such as culture media, osmolarity and osmolality are functionally equivalent; thus, here, the more common osmolarity (usually in units of mOsm = mM osmotically active solutes per liter) will be used.

The osmotic pressure of a solution is defined as the driving force developed by the

difference in water concentration between a particular solution in question and pure water. Solutions with the same osmolarity (concentration of osmotically active solute particles) will exert the same osmotic pressure, even though the solute particles may differ. These solutions are termed isosmotic. A solution having a greater concentration of solute particles than another is referred to as hyperosmotic with respect to the more dilute solution. A more dilute solution, which would exert a lower osmotic pressure, is termed hypoosmotic.

Tonicity, in contrast, describes the effect of osmolarity on cell volume. A distinction between tonicity and osmolarity is necessary because the effect of a given solute on osmotic water movement across a cell membrane depends on the membrane permeability to the solute. For example, a solution is said to be isotonic if it produces no change in the volume of a cell when placed in it (impermeable solute concentration of solution and of cell are said to be equal). While a solution is said to be hypertonic if it causes the cell to shrink (impermeable solute concentration of the solution is greater than the impermeable solute concentration inside the cell) and hypotonic if it swells (impermeable solute concentration of the solution is smaller than the impermeable solute concentration inside the cell).

Membrane Permeability

Solute transport into a cell can be mediated via two different general classes of mechanisms: channels/pores or carriers/pumps. Channels are transmembrane proteins, consisting functionally of a pore--an aqueous channel which spans the membrane--and some selectivity mechanism that allows only a specific subset of ions to permeate the channel. There is also almost universally a gating mechanism for each channel, allowing regulated switching between open and closed states in response to various stimuli. Channels are gated, variously, by binding of a specific ligand, alteration of membrane potential or mechanical stimuli such as stretch or cell volume changes. Gating may be directly mediated by these stimuli, or may be indirect, via second messenger systems including intracellular Ca^{++}, G protein signalling, or kinase pathways.

Channel selectivity is based primarily on the size and the charge of the ion. The size of the aqueous pore determines the maximum size of the compound which can permeate the channel. However, there is not a large variation in the linear dimensions of ions and small molecules. For example, a single unhydrated Cl^- ion has a diameter of about 3.6 Å, and a K^+ ion has a diameter of 2.6 Å, while a taurine molecule, containing 14 atoms, has dimensions of 4.0×4.6×7.0 Å (Strange and Jackson, 1995). Thus, taurine, K^+, and Cl^- could all permeate through a channel whose minimum diameter is 4.6 Å or greater if no other selectivity mechanisms exist. The size of the channel confers some

selectivity, but is not its sole determinant. The charge within the aqueous pore of the channel is the other main property of the channel which allows selectivity. Channels with mostly negative charge in the pore will select for positive ions and vice versa. Thus, the combination of the physical dimensions of the aqueous channel and the charge in the pore determines the selectivity of the channel.

For an ion to translocate across the membrane, an open channel is generally not required to undergo major conformational changes. In contrast, carriers/pumps must undergo a cycle of binding and conformational change. The driving force for net solute movement mediated by a carrier may be provided by a concentration gradient maintained (using energy) by the cell, or directly by ATP hydrolysis, depending on the particular carrier. Many carrier mechanisms transport more than one substrate at a time (e.g., the Na^+-K^+ ATPase). In cotransport, the carrier transports two or more different substrates in the same direction simultaneously, either into or out of the cell. In countertransport, some substrates move into the cell while others move out. For all carrier-mediated transport, it is the specific binding of ions or organic substrates to integral membrane proteins that facilitates their movement across the cell membrane. Each carrier protein in the cell membrane is selective for what substances it will bind and transport. The rate of transport into or out of the cell is limited by the concentration of available substrate, the number of carrier proteins, and the maximum rate at which each carrier protein can

operate. When all the available carrier molecules are operating at maximum speed, the carrier system is said to be saturated. At saturation, because no more carrier proteins are available and the existing ones cannot work any faster (barring any change in the transporters themselves), the net rate of transport cannot increase, regardless of the size of the concentration gradient. In contrast, it is more difficult to saturate channels, as each individual channel, in the open state, will generally allow a much larger number of substrate molecules to permeate per unit time than carriers. Thus, a lack of saturability within a reasonable physiological range of substrate is more likely to indicate transport by channels than by carriers. It should be noted, however, that even channels would be saturated by a large enough concentration of substrate.

Regulatory Volume Increase

Shrinkage under hypertonic conditions leads to changes in cellular osmolyte concentrations, changes in cell shape, disturbance of cellular metabolism as reaction rates are altered by changing concentrations of substrates, and, by way of changes in hydration status, alterations in the osmotic contribution of cellular macromolecules. These changes can lead to decreased cell viability (Hallows and Knauf, 1994; McCarty and O'Neil, 1992). Mammalian cells generally regulate their volume in order to maintain a homeostatic state when exposed to varying external or internal osmolarities.

Maintenance of their volume is accomplished by adjusting the intracellular content of osmotically active solutes (Hallows and Knauf, 1994; McCarty and O'Neil, 1992). Normally, these processes correct small deviations around the ideal volume. However, these corrections are more easily observed as recoveries from large volume changes.

Recovery from hypertonic shrinkage is termed a regulatory volume increase (RVI). Primary RVI is defined as a recovery which occurs after a direct transition to hypertonic medium. While a few cell types (e.g., some marine animal, plant, bacterial, fungal, and protist cells) can perform primary RVI, most cells lack the ability to regulate volume in such hyperosmotic media (Hallows and Knauf, 1994; Hoffman and Simonsen, 1989). However, most cells having previously recovered from hypotonically induced swelling can regulate their volumes against shrinkage when exposed to a nearly isosmotic media. Studies in avian red blood cells, epithelial cell types such as Madin-Darby canine kidney (MDCK) cells, and Ehrlich ascites tumour cells (Geck and Pfeiffer, 1986; Hoffman, 1985; Levinson, 1990; McCarty and O'Neil, 1992) have extensively shown this process of recovery from a volume decrease in isosmotic media; it is termed secondary RVI (Hallows and Knauf, 1994; McCarty and O'Neil, 1992). The mechanisms used for recovery from such an "isosmotic" shrinkage (Hallows and Knauf, 1994) are likely the physiological mechanism used in correcting small volume deviations which occur normally in the life of the cell.

In mammalian cells, RVI generally involves the uptake of NaCl and sometimes KCl, mediated either by shrinking-activated Na^+/H^+ and HCO_3^-/Cl^- exchangers (carrier proteins) coupled by their opposing effects on intracellular pH (e.g., in MDCK cells), and/or by a Na^+, K^+, $2Cl^-$ cotransporter (e.g., in Amphiuma red blood cells, some epithelial cell types such as Necturus gallbladder cells, and lymphocytes; Cala, 1983; Lopes and Guggino, 1987). The increased intracellular content of the NaCl and/or KCl causes the cell volume to increase.

However, because the increase in cell volume is mediated by increased NaCl and/or KCl transport, the cell will have a higher concentration of salt after RVI. As discussed above, increased intracellular ionic strength is detrimental to cells. Thus, for long-term regulation, many cell types (e.g., MDCK cells, Ehrlich ascites tumour cells, T lymphocytes, neurons) replace such inorganic salts with "organic osmolytes" (Chamberlin and Strange; 1989; Garcia-Perez and Burg, 1991; Law, 1991; Lee and Deutsch, 1993; McCarty and O'Neil, 1992; Yancey, 1994; Yancey et al., 1982). Many types of cells maintain nearly constant volumes and nearly constant intracellular ionic strengths by varying the intracellular osmolarity via adjustments in the concentration of organic osmolytes. A number of specific transporters have been identified which mediate the regulated uptake of organic osmolytes, including a betaine transporter (BGT), a taurine transporter (TAUT/NCT), and a broad-scope neutral amino acid transporter

(System A). However, a discussion of these and their specific functions and regulation is beyond the scope of this thesis.

Regulatory Volume Decrease

Recovery from hypotonic swelling is termed a regulatory volume decrease (RVD). Cell swelling generally involves changes in cell size, hydration status, ion and water content. Most mammalian cells, e.g., epithelial cells (Botchkin and Matthews, 1995; MacLeod et al., 1992; Ueda and Steinberg, 1994), renal cells (Carmines, 1995; Seki et al., 1995; Weiss and Lang, 1992), HSG cells (Fatherazi et al., 1994), myelocytic cells (Gallin et al., 1994), neuroblastoma cells (Lippman et al., 1995), lymphocytes (Schumaker et al., 1995), and endothelial cells (Van Renterghem et al., 1995), can regulate their volume after hypotonic swelling. KCl efflux is generally used to drive RVD. In some mammalian cells (e.g., erythrocytes), KCl is exported via a K^+/Cl^- cotransporter which is stimulated by cell swelling (Hallows and Knauf, 1994; Sakardi and Parker, 1991). However, in most nucleated mammalian cells, KCl efflux occurs through two separate pathways which are functionally coupled: a K^+ channel and an anion channel, at least one of whose conductance is increased after cell swelling (Carmines, 1995; Fatherazi et al., 1994; Foskett, 1994; Hallows and Knauf, 1994) (Figure 5).

Figure 5

Schematic diagram of RVD

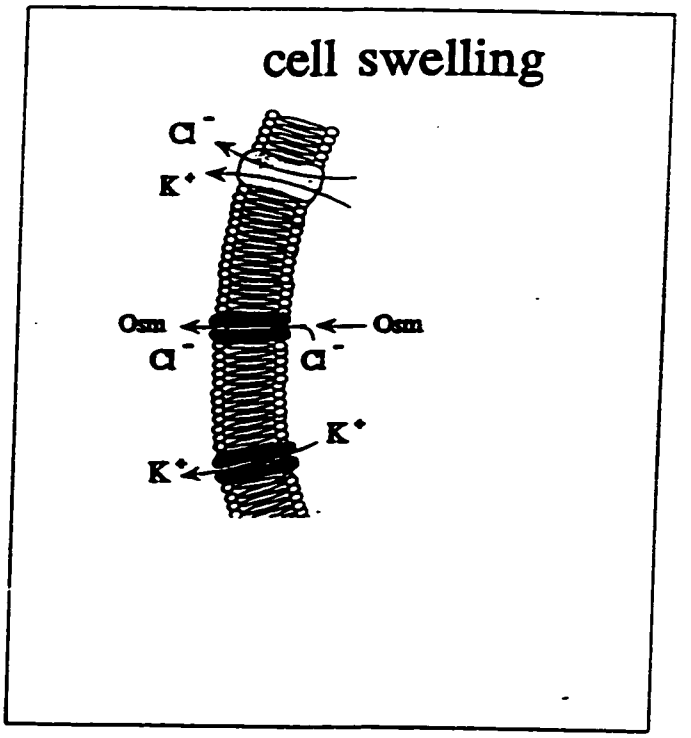
cell swelling
Cl⁻
K⁺
Osm
Osm
Cl⁻
Cl⁻
K⁺
K⁺

Characteristics of K^+ and Cl^- Channels in RVD

Potassium (K^+) channels play important roles in the maintenance of cell volume in numerous excitable and non-excitable cells. There exist several different K^+ channel subtypes which regulate different physiological processes, e.g., delayed-outward rectifiers, transient-outward rectifiers, anomalous or inward-rectifiers, and Ca^{++}-activated K^+ channels. Only intracellular Ca^{++} regulates the last type. Only inwardly-rectifying K^+ channels (Ca^{++}-independent) and Ca^{++}-activated K^+ channels have been shown to be implicated in RVD (see below).

There are at least two forms of Ca^{++}-dependent K^+ channels that are recognized. These forms differ in unit conductance, in voltage and Ca^{++} sensitivity, and in pharmacology. The SK, or low conductance Ca^{++}-dependent K^+ channels, are inhibited by the bee venom toxin apamin (but not charybdotoxin, an inhibitor of the other major Ca^{++}-dependent K^+ channel subtype (see below)). These channels have a small unitary conductance (6-22 pS), negligible voltage sensitivity, and are involved in the after-hyperpolarization of action potentials (Castle et al., 1989; Kolb, 1990). The BK, or large conductance Ca^{++}-dependent K^+ channels, are sensitive to the scorpion toxin charybdotoxin, but not apamin. These channels have a larger unitary conductance (100-250 pS) and are activated by both variations in intracellular Ca^{++} and depolarization (Castle et al., 1989; Kolb, 1990). Apamin has been shown to inhibit low conductance

Ca^{++}-dependent K^+ currents (IC_{50}=1-10 μM) in cultured rat myocytes (Moczydlowski et al., 1988), intestinal smooth muscle (Maas et al., 1980; Weir and Weston, 1986) and hepatocytes (Burgess et al., 1981; Cook et al., 1983). Charybdotoxin has been shown to inhibit large conductance Ca^{++}-dependent K^+ permeability (IC_{50}= 2-100 nM) in cultured kidney epithelial cells (Guggino et al., 1987), rat aortic smooth muscle cells (Talvenheimo et al., 1988), and rat glioma cell line C6 (Tas et al., 1988).

There are three possible volume-sensitive anion (Cl^-) channel types identified to date in animal cells: outwardly-rectifying channel, a ClC family channel which is possibly ClC-2 or ClC-3, and the maxi channel (Duan et al., 1997; Strange et al., 1996). Of the three anion channels, only the ClC channels are identified at the molecular level (see below). ClC-2 is a protein composed of 907 amino acids with a calculated molecular mass of 99 kDa (Pusch and Jentsch, 1994; Strange et al., 1996), and the ClC-3 subtype is similar (Duan et al., 1997). Although two of the putative volume-sensitive channels remain molecularly unidentified, all three volume-sensing anion channels possess unique characteristics with regards to their anion selectivity, their activation and their inhibition (Strange et al., 1996).

The outward-rectifying channel has been described to be selective for $SCN^- > I^- > NO_3^- > Br^- \cong Cl^- > F^-$ > gluconate and it is said to be activated by osmotic swelling or by a volume increase induced by fluid injection into the cell (Strange et al., 1996). In virtually

all mammalian cells studied to date, cell swelling activates an outwardly-rectifying anion conductance. The channel underlying this conductance appears to be distinct from other volume-activated Cl^- channels since it is also permeable to organic substrates (Strange et al., 1996), mediating not only current carried by anions, but also apparently being responsible for the efflux of organic osmolytes upon cell swelling. Characterization of the swelling-activated efflux pathway has been carried out mainly in mammalian cells and cells of lower vertebrates (Banderali and Roy, 1992; Hallows and Knauf, 1994; Jackson and Strange, 1995; Kirk et al., 1992). The effluxes of amino acids, polyols, and methylamines from these various cell types all share the common characteristics of being mediated by passive, Na^+-independent transport pathways that do not exhibit saturation behaviour (see channel definition above) (Banderali and Roy, 1992; Strange et al., 1996). This efflux pathway is inhibited by the same range of compounds which block the swelling-activated current: stilbenes (e.g., DIDS), NPPB, extracellular ATP, fatty acids, lathanum and tamoxifen (Strange et al., 1996). These findings have led to the general conclusion that diffusion through membrane channels, rather than saturable carrier-mediated transport, is responsible for organic osmolyte loss (Strange et al., 1996). The channel responsible for this activity has been termed the Volume Sensitive Organic osmolyte/Anion Channel (VSOAC) and may be identical to the ClC-3 isoform of Cl^- channel (Duan et al., 1997; Strange et al., 1996, see below).

The ClC-2 channel, on the other hand, has been described to be selective for $Cl^- \cong Br^- > I^-$ > cyclamate (Strange et al., 1996). Activation is said to be provoked by osmotic swelling and hyperpolarization (e.g., rat brain, Xenopus oocytes) and is inhibited by A9C, DPC, with little effect of the stilbene DIDS (Pusch and Jentsch, 1994; Strange et al., 1996; Thiemann et al., 1992). The activation of endogenous ClC-2 by swelling has not been observed in intact cells and no volume regulatory role for the channel has been demonstrated. However, given the widespread distribution of ClC-2 in mammalian cells and tissues, ClC-2 is suggested to play an important role in an essential "housekeeping" function (Strange et al., 1996).

Finally, the maxi channel has been described as selective for Cl^- > acetate $\cong HCO_3^-$. It is activated by osmotic swelling, membrane stretch, patch excision, protein kinase C (PKC), cytochalasins, phorbol esters and is inhibited by phalloidin, DIDS, NPPB, pertussis toxins and inhibitors of PKC (Strange et al., 1996).

Calcium Signalling in RVD

The cellular signalling and regulatory pathways underlying solute and volume regulation in many cell types require changes in intracellular Ca^{++}. Ca^{++} signalling in human lymphocytes, osteosarcoma cells, rabbit renal PST, has been proposed to be a key component of recovery from hypotonic swelling (Brugnara, et al., 1993; Foskett, 1994;

Grinstein et al., 1986; Grinstein et al., 1982; McCarty and O'Neil, 1992; Neufield et al., 1983; Yamaguchi et al., 1989). In these models, the K^+ or Cl^- conductance is activated by a swelling-induced rise in intracellular Ca^{++}. It is not clear how Ca^{++} performs its function in modulating RVD. It is possible that the K^+ and/or Cl^- conductance is not directly activated by Ca^{++} but indirectly activated through the operation of another Ca^{++}-dependent process, i.e., calmodulin, production of secondary intracellular messenger such as DAG, the exocytic insertion into the plasma membrane of vesicles containing ion channels, or the phosphorylation and dephosphorylation of existent transporters (Geck and Pfeiffer, 1986; Hoffman, 1985; Jennings and Schultz, 1991; Kaji and Tsukitani, 1991; Sukudi et al., 1990). Yet, because no one has reported a mechanism for control of RVD by Ca^{++} at the outer face of the membrane, it is widely assumed that extracellular Ca^{++} serves to supply intracellular Ca^{++} and that the regulatory role of Ca^{++} is asserted at an intracellular site (Brugnara et al., 1993; McCarty and O'Neil, 1992). Evidence has been presented that Ca^{++} entry across the plasma membrane may be supplemented by, or even replaced by Ca^{++} released from intracellular stores (McCarty and O'Neil, 1992). If Ca^{++} released from internal stores were sufficient to support activation of the ion conductance in a given cell, RVD in that cell would not be dependent on external Ca^{++} (McCarty and O'Neil, 1992). The mitochondria and the endoplasmic reticulum are plausible intracellular storage sites for swelling-activated Ca^{++} release (Brugnara et al., 1993; McCarty and O'Neil, 1992).

How cell swelling is transduced into a release of Ca^{++} from these storage sites is unknown but it is possible that it is caused by changes in voltage across the membrane or stretch of the membrane or cytoskeleton.

Although many cell types have been shown to utilize Ca^{++} signalling in the process of RVD, this dependence is not universal. Some cell types, e.g., Ehrlich ascites tumour cells and clonal N1E115 neuroblastoma cells, have been shown to use Ca^{++}-independent K^+ and Cl^- conductances and not require changes in intracellular Ca^{++} for RVD (Foskett, 1994; Grinstein et al., 1982; Hoffman, 1985; Lippman et al., 1995; McCarty and O'Neil, 1992). It is possible that RVD is not regulated solely by any one pathway, but that recovery involves the interaction of several signalling pathways, each of which may exert variable control of the different modulator pathways involved in RVD (McCarty and O'Neil, 1992). Some cell types were shown to undergo RVD even when intracellular Ca^{++} was depleted by preincubation with external EGTA plus the Ca^{++} ionophore ionomycin, or buffered at a low level by loading the cell with the Ca^{++} chelator BAPTA, arguing against the involvement of Ca^{++}-dependent conductance or channels, or Ca^{++} signalling, in RVD in these cells. Many authors proposed swelling-induced K^+ loss might occur via Ca^{++}-independent K^+ channels that may be voltage activated or stretch activated during swelling (see above) in such cells. Others propose that K^+ efflux passively follows Cl^- efflux after Cl^- channel activation as required to balance charge.

Permeability of Organic Osmolytes in RVD

The process underlying volume control after swelling invariably requires redistribution of intracellular osmolytes, allowing water to follow by osmosis. Volume recovery is generally achieved by regulating the fluxes of inorganic ions. However, the efflux of organic osmolytes often plays a major role in volume regulation, explaining the existence of swelling-activated organic osmolyte channels (Banderali and Roy, 1992; Chamberlin and Strange, 1989; Gallin et al., 1994; Jackson and Strange, 1995; Kirk et al., 1992; Kwon and Handler, 1995). Free amino acids and other organic solutes serve as important osmolytes (Hallows and Knauf, 1994; Kirk et al., 1992; Kwon and Handler, 1995). Many of these organic solutes (e.g., glycine, taurine) are present in millimolar concentrations in the cytoplasm and are available in sufficient quantities for cellular osmoregulation in many cases (Dawson and Baltz, 1997; Van Winkle et al., 1994; Van Winkle et al., 1990). Some of these organic osmolytes (e.g., taurine) may also perform other important functions such as protecting the cells from oxidative stress, and stabilization of membranes (Hallows and Knauf, 1994; Kirk et al., 1992; Kwon and Handler, 1995). The loss of organic osmolytes in hypotonic conditions was poorly understood until recent studies indicated that structurally dissimilar organic osmolytes are lost from cells via the swelling-activated anion channel (see above) (Banderali and Roy, 1992; Chamberlin and Strange, 1989; Hallows and Knauf, 1994; Jackson and Strange,

1995; Okada, 1997; Strange et al., 1996).

In some cells, e.g., rat C6 glioma cells, astrocytes and intestine 407 cells, the swelling-activated anion (Cl^-) channel used in RVD appears to be fairly non-selective; it is permeable not only to Cl^-, but also to a broad range of organic osmolytes (e.g., taurine, glycine, betaine) (Banderali and Roy, 1992; Hallows and Knauf, 1994; Jackson and Strange, 1995; Okada, 1997; Strange et al., 1996). This activity is said to be mediated via the specific type of channel designated as the Volume-Sensitive Organic osmolyte/Anion Channel (VSOAC), or Volume-Sensing, Outwardly Rectifying (VSOR) channel (Jackson and Strange, 1995; Okada, 1997; Strange et al., 1996).

Jackson and Strange (1995) have reported the VSOAC in C6 glioma cells to be inhibited by millimolar concentrations of extracellular ATP. The physiological significance of this inhibition, if any, is uncertain. However, studies in C6 glioma cells have demonstrated that inhibition by extracellular ATP increases open-channel noise (indicating a direct block of the channel in the open state), is voltage dependent, and is sensitive to the direction of net Cl^- flux through the channel (Jackson et al., 1996). Conversely, swelling-induced activation of the VSOAC in mammalian cells requires intracellular, nonhydrolytic ATP binding (Jackson and Strange, 1995). At present, it is unclear whether cytosolic ATP binds to and directly modulates the channel itself at an intracellular site and/or to accessory regulatory proteins (Jackson et al., 1996; Jackson

and Strange, 1995). Nonetheless, intracellular ATP probably modulates the effects of volume regulation in cell types that use a VSOAC-like channel (Jackson and Strange, 1995). The VSOR has similar properties to the VSOAC, such as its physiological dependency on cytosolic ATP and biophysical characteristic as a voltage-dependent single channel conductance (Okada, 1997) and thus might be identical.

In addition, a cloned member of the ClC family of chloride channels (ClC-3) has recently been found to have similar properties to the VSOAC/VSOR, indicating that ClC-3 may be the protein functioning as the swelling-activated anion/osmolyte channel (Duan et al., 1997). The protein encoded by the gene for ClC-3, cloned previously from rat kidney, mouse liver, and human fetal brain, has a similar hydropathy profile to other ClC family members, but, uniquely, Cl^- currents expressed from rat ClC-3 in Xenopus oocytes are outwardly-rectifying, more permeable to I^- than Cl^-, and inhibited by PKC, stilbene derivatives such as DIDS and external ATP (Duan et al., 1997). These properties are strikingly similar to the swelling-activated Cl^- channels found in studies in the heart (Duan et al., 1997; Duan et al., 1995), but the regulation of ClC-3 by cell volume has not been fully tested nor has the presence of ClC-3 in the full range of cells with VSOAC/VSOR currents been demonstrated.

Nucleotides and RVD: Purinergic Receptors

The ability of external ATP to block VSOAC currents would imply that RVD should be inhibited by external ATP. However, there is the alternative possibility that external ATP could activate an ATP receptor or purinergic receptor (Burnstock, 1985; Fredholm et al., 1994; Kenakin et al., 1992) on the cell surface, with only an indirect effect on RVD rather than directly acting on any VSOAC/VSOR channel (see above).

Burnstock (1978) originally suggested purinergic receptors could be subgrouped into two subclasses, P_1 and P_2. This classification was based on four criteria: a) comparison of the relative potencies of ATP, ADP, AMP, and adenosine; b) observation of the selective actions of antagonists, in particular the methylxanthines; c) modulation of the adenylate cyclase by adenosine but not ATP; and d) induction of prostaglandin synthesis by ATP but not adenosine (Burnstock, 1978; Dalziel and Westfall, 1994; Kwon and Handler, 1995). Purinoreceptors classified as P_1 (adenosine receptors) are more responsive to adenosine and AMP than to ADP and ATP, and methylxanthines such as theophylline and caffeine are antagonists of these receptors (Burnstock, 1978; Dalziel and Westfall, 1994). In addition, stimulation of P_1 purinoreceptors (A_1, A_{2a}, A_{2b}, A_3) (Table 1) leads to the modulation of adenylate cyclase activity (for A_2 receptors only) (Fredholm et al., 1994). P_2 purinoreceptors (ATP receptors), on the other hand, are more responsive to ATP and ADP than AMP and adenosine, are not antagonized by methylxanthines, and do

not modulate the adenylate cyclase system. Their stimulation is generally accompanied by prostaglandin synthesis (Burnstock and Kennedy, 1985; Burnstock, 1978). P_1 purinoreceptors have been classified to be generally coupled to a G-protein effector system whereas P_2 purinoreceptors can either be coupled to a G-protein effector system (P_{2Y}, P_{2U}, P_{2T}, P_{2D}) or be intrinsically an ion channel (P_{2X}) or a nonselective pore (P_{2Z}) (Table 2) (Fredholm et al., 1994).

Table 1

Classification of P_1 Purinoreceptors

Adapted from Fredholm et al. (1994).

Name	A_1	A_{2A}	A_{2B}	A_3
Types	G-protein coupled	G-protein coupled	G-protein coupled	G-protein coupled
Distribution	Brain, testis, adipose tissue, heart, kidney	Brain	Wide, high in gastrointestinal tract	Testis
Effectors	Decrease cAMP; increase IP_3; increase K^+; decrease Ca^{++}	Increase cAMP	Increase cAMP	Decrease cAMP

Table 2

Classification of P_2 Purinorecptors

Adapted from Fredholm et al. (1994).

Name	P_{2X}	P_{2Y}	P_{2U}	P_{2T}	P_{2Z}	P_{2D}
Types	Intrinsic ion channel	G-protein coupled	G-protein coupled	G-protein coupled	Nonselective pore	G-protein coupled (?)
Distribution	Smooth muscles, brain, heart, spleen	Wide distribution	Wide, found in many cultured cells and in vascular muscle	Platelets	Mast cells, macrophages, vas deferens	Chromaffin cells, rat brain synaptoso-mes
Effectors	Na^+, K^+, Ca^{++}	Increase IP_3/Ca^{++}/ DAG; decrease cAMP	IP_3/Ca^{++}/ DAG; Ca^{++}, Cl^-, and K^+ currents	IP_3/Ca^{++}/ DAG; cAMP	Na^+, K^+, Ca^{++}	Increase Ca^{++}

RVD in Mouse Zygotes

The role cell volume regulation plays in preimplantation embryo development in vitro has recently begun to be explored. It is known that embryos will tolerate the large transient volume changes associated with cryopreservation (Oda et al., 1992) but no volume regulation seems to be involved in this tolerance. Under more physiological conditions, Van Winkle, et al. (1994) reported that mouse zygotes recovered from hypotonic swelling but only very slowly ($t_{1/2}$ = 90 min). In contrast, measurements conducted throughout my Honour's project (Séguin, 1996) have shown that RVD can, in fact, occur more quickly ($t_{1/2}$ = 7-10 min) at the zygote stage. Significant inhibition of recovery was observed in the presence of several different Cl^- channel inhibitors (DIDS, A9C, IAA-94, NPPB) as well as K^+ channel inhibitors (barium, quinine), suggesting that the embryos required KCl efflux through Cl^- and K^+ channels to perform RVD (Séguin and Baltz, 1997; Séguin, 1996). The channels appeared to be separate entities since the cation ionophore gramicidin, selective for K^+ and Na^+, restored RVD when the K^+ channels were blocked with quinine, but not when the Cl^- channels were blocked with DIDS (Séguin and Baltz, 1997; Séguin, 1996).

Clotrimazole, a compound which has been shown to be effective at blocking the Ca^{++}-dependent K^+ channel in erythrocytes (Brugnara et al., 1993), but which may also block other K^+ channels with lower affinity, showed a partial inhibition of mouse zygote

RVD (Séguin and Baltz, 1997; Séguin, 1996). Clotrimazole has been found to completely block the charybdotoxin-sensitive, Ca^{++}-dependent K^+ channel in erythrocytes with an IC_{50} of well under 100 nM (Brugnara et al., 1993). Since clotrimazole only demonstrated a partial inhibition on RVD in the zygote at a concentration of 10 μM, it was concluded that the erythrocyte-type Ca^{++}-dependent K^+ channel was not likely required for zygote RVD (Séguin and Baltz, 1997). The possibility remained that another subtype of a Ca^{++}-dependent K^+ channel could be mediating RVD. The question of whether Ca^{++} signalling was required in mouse zygote RVD remains unknown and constitutes an objective of this thesis.

The type of Cl^- channel that regulates mouse zygote RVD also remains unknown. Since preimplantation embryos require organic osmolytes throughout development and given the evidence of outward-rectifying anion channels, which are permeable to anions and organic osmolytes, in many mammalian cell types, it is hypothesized that the swelling-activated Cl^- channel found in mouse zygotes could also be permeable to organic osmolytes.

3. Objectives and Hypotheses

The objectives of this thesis were:

1) To examine the possible involvement of intracellular Ca^{++} in signalling or Ca^{++}-

dependent K^+ channels in mouse zygote RVD, and

2) To determine whether the swelling-activated anion channel is permeable to organic osmolytes.

Objective 1: Involvement of Ca^{++} in RVD

An increase in intracellular Ca^{++} has been shown to be required in RVD in some cell types, while RVD is independent of intracellular Ca^{++} in others (see above). Thus, no *a priori* assumptions could be made about Ca^{++} signalling in mouse zygotes.

A working hypothesis was that:

Swelling induced an increase in intracellular Ca^{++} concentration in mouse zygotes, and that this increase was required for RVD.

Approach:

The first step in the investigation consisted of testing whether hypotonic swelling, under the same conditions that elicited RVD in zygotes (Séguin and Baltz, 1997), caused an increase in intracellular Ca^{++} concentration. The measurement of intracellular Ca^{++} during swelling required the use of a ratiometric Ca^{++}-sensitive fluorophore, fura-2, which was loaded by incubation into the cytoplasm of the zygote. To confirm that any apparent increase in Ca^{++} measured by fluorescence imaging was indeed reporting an actual increase in Ca^{++} rather than being an artificial effect of swelling on fluorescence, the Ca^{++}

chelator, BAPTA-2, loaded intracellularly, was used to confirm that any apparent increase in Ca^{++} could be abolished or attenuated.

To then determine if any observed increase in Ca^{++} was required for RVD, RVD was measured in the presence and in the absence of BAPTA. It was assumed that if an increase in Ca^{++} were required for RVD to occur, then RVD would be inhibited when BAPTA was present, since the chelator would largely eliminate any increase in intracellular Ca^{++}.

Another working hypothesis was that:

Ca^{++} might act via Ca^{++}-dependent K^+ channels in mouse zygotes.

Approach:

To determine whether known types of Ca^{++}-dependent K^+ channels might be required for RVD in mouse zygotes, the effect of specific pharmacological inhibitors of small (SK) and large (BK) conductance subtypes were tested. It has been shown that clotrimazole had a partial effect on RVD (Séguin and Baltz, 1997; Séguin, 1996). However, this partial inhibition with clotrimazole was at a much higher concentration than that which had previously been described to completely inhibit the large conductance subtype in erythrocytes (Brugnara et al., 1993). Nonetheless, it was still possible that either a small conductance subtype of the channel was active, or that a variant of the large conductance subtype which was insensitive to clotrimazole was present. Therefore, specific

concentrations of the Ca^{++} -dependent K^+ channel blocker, apamin and charybdotoxin, which have indicated known positive effects in other cell types, were employed. Apamin is a component of bee venom which specifically blocks the small conductance subtype (see above), whereas charybdotoxin is a component of scorpion venom which specifically blocks the large conductance subtype (see above). By assessing the effect of each of these channel blockers on zygote RVD, it can be ascertained whether either of these Ca^{++} -dependent K^+ channels might be required.

Objective 2: Permeability of Organic Osmolytes

Mouse zygotes have been shown to require organic osmolytes in order to maintain viability when cultured in medium with moderately increased osmolarity (Dawson and Baltz, 1997; Van Winkle et al., 1994). In addition, studies have shown that mouse zygotes accumulate the organic osmolyte glycine to provide intracellular osmotic support, and to maintain cell volume (Dawson et al., 1998). Therefore, it would be likely that the release of such accumulated osmolytes would be a feature of RVD in mouse zygotes, and a normal part of their volume regulation. In a number of cell types, the swelling-activated increase in permeability to organic osmolytes is due to a permeability of a single type of swelling-activated anion channel (VSOAC) to a range of organic compounds (Okada, 1997; Strange et al., 1996).

Two working hypotheses were that:

The permeability to a number of organic compounds increases upon hypotonic swelling in zygotes, and, organic osmolytes permeate via the swelling-activated anion channel found in mouse zygotes.

Approach:

A similar assay as the one developed by Passantes-Morales et al., (1993) was used, which allowed the screening of a large number of compounds for increased permeability in hypotonically swelled zygotes. This assay consisted of introducing a large concentration of each suspected osmolyte in the external medium during experimentally induced hypotonic swelling. If the potential osmolyte were highly permeable, then RVD would be blocked due to a "backflux" of osmolyte through swelling-activated pathway. As an osmolyte enters the cell, driven by the large imposed concentration gradient; it opposes the effect of any intracellular osmolytes which must be released upon cell swelling to allow RVD. Thus, this assay allowed the rapid screening of a large number of compounds for swelling-activated permeability, flagging their permeability through the swelling-activated anion channel.

As an independent test for a swelling-activated permeability to organic osmolytes in zygotes, the organic compound glycine, which has been shown to have a role as an "osmolyte" in zygotes (Dawson et al., 1998; Dawson and Baltz, 1997), and which was

identified in the first set of experiments (the "backflux" approach) as a highly-permeable compound, was used to directly demonstrate that permeability is directly increased upon cell swelling. This was done by examining whether the rate of influx of ^{3}H glycine was increased upon hypotonic swelling increased upon swelling.

To determine if any swelling-activated increase in permeability of organic compounds in zygotes was due to their permeation through a swelling-activated anion channel with similar properties to those described in other cells, Cl^- channel inhibitors and nucleotides (i.e., ATP at millimolar levels) previously shown to block this type of channel were used (Okada, 1997; Strange et al., 1996; Séguin and Baltz, 1997). It has been previously shown that common Cl^- channel blockers inhibited RVD in mouse zygotes (Séguin and Baltz, 1997; Séguin, 1996). Because inhibition by external ATP at millimolar levels is considered diagnostic of the VSOAC/VSOR type of swelling-activated anion/organic osmolyte channel, the effect of external ATP on RVD and on glycine permeability in the mouse zygote was examined.

A possible alternative mechanism for external ATP action on RVD would be via purinoreceptors, and so this would have to be ruled out before concluding that any effect was likely upon the swelling-activated channel itself. Since the pharmacology of purinoreceptors subtypes, especially their relative specificity for various adenosine nucleotides, is well established, the effects of several adenosine nucleotides on mouse

zygote RVD were examined. If only millimolar ATP, but not submillimolar ATP or millimolar concentrations of adenosine could block RVD, this would rule out the possibility that effects on RVD were via purinoreceptors rather than direct effects on the swelling-activated channel.

MATERIALS AND METHODS

Animals

The animals used in this study were 5-6 week old female CF-1 mice obtained from Charles River Canada (St-Constant, PQ) and maintained at the Loeb Health Research Institute. All animals had free access to water and food, and were kept on a light: dark cycle of 12 hours: 12 hours. Superovulation was induced with intraperitoneal injections of 5 IU Pregnant Mares Serum Gonadotropin (PMSG), followed 47.5-48 hours later by 5 IU human Chorionic Gonadotropin (hCG). PMSG was principally used to induce follicle growth, mimicking the gonadotropic effects of FSH whereas hCG was used to induce ovulation, mimicking the effects of LH (Figure 4).

The female CF-1 mice were subsequently caged with BDF male mice (Charles River Canada) following hCG injections and were examined the following morning for the presence of a vaginal plug. The female CF-1 mice were sacrificed by cervical dislocation 19-23 hours after injection with hCG and oviducts were removed. All animals were maintained in accordance with the Guide to the Care and Use of Experimental Animals, 2nd edition, of the Canadian Council Animal Care. In addition, the protocols used were approved by the Ottawa Hospital, Civic Campus, Animal Care Committee.

Isolation of Zygotes

The collection and handling of zygotes required a medium with a stable pH when exposed to air (see below). Most culture medium, which are bicarbonate-buffered (see below), are insufficient for maintaining embryos in air even for short periods of time (Lawitts and Biggers, 1993). Thus, a flushing-holding medium, Hepes-KSOM, was used to obtain zygotes (Lawitts and Biggers, 1993; see below for media).

Zygotes were obtained by flushing excised oviducts. Flushing consisted of filling the coiled-shape oviductal tube with Hepes-KSOM media through the opening in the fimbrae (finger-like) area of each tube. The procedure required the use of a blunted 30-gauge needle, which contained Hepes-KSOM and 300 μg/ml hyaluronidase (Sigma) added to disperse the cumulus mass which enclosed the zygotes. Flushing was done using a dissecting stereo microscope with epi-illumination provided by two fibre optic light sources.

Zygotes were washed through several drops of Hepes-KSOM, using flame-pulled, mouth-operated Pasteur pipettes. Pasteur pipettes were moulded using a small flame, into a long narrow shaft that changes diameter gradually over the flame-pulled length of the pipette. The use of a long narrow shaft of approximately 2-3 centimetres long with a gradually changing diameter and an internal diameter of 200 to 250 μm was optimal for housing the zygotes near the tip of the pipette. This reduced the chance that zygotes

would be lost in the pipette during transfers, and also lessened the amount of medium transferred with the zygotes.

Isolated zygotes were distinguished from unfertilized oocytes by the presence of two pronuclei. The presence of pronuclei was confirmed by the appearance of small, dark circular shapes found within the cytoplasmic area of the zygote when viewed under the dissecting microscope.

Media

The components (Sigma, St-Louis, MO; embryo culture or cell culture grade) of the media used in these studies were based on KSOM mouse embryo culture medium (Erbach et al., 1994; Lawitts and Biggers, 1993; Lawitts and Biggers, 1991), modified by the omission of bovine serum albumin (BSA). When required, polyvinyl alcohol (PVA; 1mg/ml) was used instead of BSA as the macromolecular component of the medium. KSOM embryo medium contained (in mM except where noted) 95 NaCl, 2.5 KCl, 0.35 KH2PO4, 0.2 MgSO4, 10 sodium-lactate, 0.2 glucose, 25 $NaHCO_3$, 1.7 $CaCl_2$, 0.01 tetrasodium ethylenediaminetetraacetic acid (EDTA), 60 μg/ml penicillin G (potassium salt), and 44 μg/ml streptomycin sulfate. KSOM was equilibrated with 5.0% CO_2 and air for a period of 24 hours before use. The pH of KSOM equilibrated at 5% CO_2/air was 7.35. The osmolarity of this solution was 238-243 mOsm as measured using a vapour

pressure osmometer (Vapro model 5520 vapour pressure osmometer, Wescor, Logan, UT).

For experiments in which zygotes were swelled, 148-153 mOsm KSOM was used in which the osmolarity was reduced by lowering the NaCl concentration from 95 mM to 42 mM. For organic osmolyte experiments, a modified KSOM was used in which the NaCl concentration had been reduced from 95 mM to 17 mM and the appropriate compound added to increase osmolarity. The additions consisted of either 50 mM of the trisaccharide D(+) raffinose, which was used as the control medium since raffinose is not transported or metabolized by mammalian cells, or 50 mM of a possible organic osmolyte to be tested. If the organic compound was only available as a Na^+ or K^+ salt, 25 mM of the salts were used instead, so that the addition was isosmotic. The measured pH and osmolarities of these media are shown in Table 3. In glycine influx experiments, sodium-depleted KSOM was used in order to prevent any Na^+-dependent uptake of the ^{3}H-glycine via the Gly transporter (Dawson and Baltz, 1997; Van Winkle et al., 1990): DL-lactic acid (pH adjusted with KOH) was substituted for sodium lactate, pyruvic acid (potassium salt) was substituted for sodium pyruvate, and choline bicarbonate ([2-Hydroxyethyl]trimethylammonium bicarbonate) was substituted for sodium bicarbonate.

For the washing and the flushing of zygotes from the oviduct, 250 mOsm

Hepes-KSOM medium was used, wherein all but 4 mM of the $NaHCO_3$ in KSOM was replaced with an equimolar amount of N-2-hydroxyethylpiperazine-N'2-ethanesulfonic acid (Hepes) free acid, and the medium adjusted to pH 7.4-7.5 at 20°C using NaOH. Zygote intracellular pH was stable and at normal value of approximately 7.1-7.2 in Hepes-KSOM, as shown by Philips and Baltz (1996).

Ca^{++}-dependent K^+ Channel Inhibitors and Nucleotides

Charybdotoxin (Research Biomedicals, Natick, MA) was dissolved in Hepes-KSOM and apamin (Research Biomedicals) was dissolved in deoxygenated water to make a 1000 x stock before use. Charybdotoxin and apamin have been reported to specifically block large-conductance Ca^{++}-dependent K^+ channels at 100 nM and small-conductance Ca^{++}-dependent K^+ channels at 1 μM, respectively (Burgess et al., 1981; Cook et al., 1983; Guggino et al., 1987; Maas et al., 1980; Moczydlowski et al., 1988; Talvenheimo et al., 1988; Tas et al., 1988; Weir and Weston, 1986). Thus, 100 nM charybdotoxin and 1 μM apamin were used to determine whether the K^+ channels required for mouse zygote RVD are likely to be of either subtype of the Ca^{++}-dependent K^+ channels.

Adenosine and cAMP (Adenosine 3':5'-cyclic monophosphate) were added directly to the medium to produce the appropriate concentration. ATP (Adenosine

5'-triphosphate) was dissolved in deoxygenated water, and pH adjusted with the addition of NaOH, to make a 1000 x stock before use.

ATP has been reported to inhibit currents through a volume-sensitive organic osmolyte/anion channel in rat C6 glioma cells and astrocytes when used at a 5 mM concentration. Thus, 5 mM ATP was initially used to determine whether the swelling-activated anion channel in mouse zygotes demonstrated the same inhibitory characteristics as the anion channels reported in rat C6 glioma cells and astrocytes. Extracellular cAMP has been described to have no effect on RVD in mammalian cell types (e.g., epithelial cells) (Tsumura et al., 1996), although a similar conductance in Xenopus oocytes has been reported to be cAMP-inhibitable (Ackerman et al., 1994). Thus, 5 mM cAMP was used to determine whether the swelling-activated anion channel in mouse zygotes demonstrated the similar characteristics as the anion channels reported to mediate RVD in mammalian cells. A second concentration of ATP, 0.1 mM, was employed to demonstrate a dose-dependent effect of ATP upon RVD. This concentration was chosen because it is below the effective range for inhibition of VSOAC currents in zygotes; inhibition of the swelling-activated current in mouse zygotes was not evident or detected with 1 mM or lower concentrations of extracellular ATP (Kolajova and Baltz, 1999). In contrast, 0.1 mM ATP would be expected to fully activate the ATP selective purinoreceptor subtype. Thus, the choice of 5.0 mM and 0.1 mM ATP would distinguish

between the possible mediation of any effect of ATP on RVD via direct action on a swelling-activated channel, or via purinoreceptors. Similarly, 5 mM adenosine was used to determine whether mouse zygote RVD could be mediated through a purinoreceptor of the adenosine-selective subtype. While 5 mM adenosine fully activates the purinoreceptor, this concentration would have no effect on the swelling-activated channel.

Number of Zygotes Per Experiment

Data were obtained simultaneously from pooled zygotes of three mice. A number of zygotes were handled together and subjected to exactly the same treatment. Replicates were performed with such pools of zygotes on separate days. Zygotes obtained from different mice on separate days were physiologically indistinguishable (approximately 3% variance in RVD data between days). Throughout, "n" indicates the total number of zygotes in a given treatment group, while "N" indicates the number of replicates. For example, n = 23, N = 3 indicates that the data was obtained from a total of 23 individual zygotes on 3 separate days.

Viability was confirmed by visually monitoring each zygote's colour, shape, and dimensions throughout each experiment. Zygotes which demonstrated any membrane blebbing or rupture, membrane folding, cytoplasmic granulation, and darkening of colour

(i.e. from yellow to brown) were considered to be non-viable and were excluded from experimental analysis (approximately 1-2% of zygotes overall were judged non-viable and excluded).

Measurement of Recovery from Cell Swelling

Randomly chosen zygotes (between 5-15) were transferred to a temperature-controlled chamber (37°C ± 0.5°C; Biophysica, Baltimore, MD) filled with Hepes-KSOM. This chamber was comprised of two square pieces, an aluminum base and a Teflon upper piece that, when screwed together, made a 'sandwich' which held a round cover glass that formed the bottom of a chamber. The chamber, when assembled, held approximately 2.5 ml. The sides of the chamber were formed by a silicon rubber-enclosed heating coil which maintained the temperature. The chamber, once assembled was mounted on the stage of a Zeiss Axiovert inverted microscope. Zygotes attached firmly to the clean cover glass bottom of the chamber in protein-free media without any special manipulations or treatments.

Zygotes were abruptly swelled by exchanging the room-temperature (22°C) Hepes-KSOM medium in the chamber reservoir for 37°C hypoosmotic KSOM, maintained under a humidified 5% CO_2 and air. Solutions were exchanged by flushing the 2.5 ml chamber with 30 ml of prewarmed solution equilibrated with 5% CO_2 and air.

Medium was added at a constant rate of about 0.75 ml/sec using a syringe driver to slowly expel medium from a 30 ml, prewarmed, medium-filled syringe, connected by tubing to an outlet at the side of the chamber. An aspirator was connected to an outlet for medium, which was placed in the chamber near the top and at the side opposite from the medium inlet. Thus, a constant flow from one side of the chamber to the other was maintained during medium exchanges. It had been previously confirmed, using tracer dyes, that medium replacement was virtually complete using this setup. Medium exchange took approximately 45-60 seconds.

A 5% CO_2/air atmosphere was maintained in the chamber by a constant flow of 5% CO_2/air into the top of the covered chamber. The gas was introduced at 100% humidity, which was required to prevent significant evaporation of the 2.5 ml medium sample and hence changes in osmolarity (Séguin and Baltz, 1997; Séguin, 1996). Humidification of the gas was accomplished by bubbling the gas mixture through deionized/distilled millipore water at 65-70°C; cooling which occurred in the tube between the water and the chamber resulted in introduction of appropriately warm, humid gas.

A videomicroscopy system built around the Zeiss Axiovert inverted microscope was used to record each experiment (Zhao et al., 1995). Images were monitored using a solid-state video camera (CCD72, DAGE-MIT, Michigan City, IN) (Zhao et al., 1995).

The imaging system was controlled by *isee* and *dsp/os* software and imaging hardware (Inovision Inc., Durham, NC) with a Silicon Graphics Indigo2 (R4400, Extreme Graphics) Unix workstation (Silicon Graphics, Mountain View, CA) (Zhao et al., 1995). Bright field images were obtained using the microscope condenser with the tungsten illumination attenuated by a 2.0 O.D. neutral density filter.

The quantitative imaging system was used to determine the diameter of each zygote as a function of time. The zygotes were imaged using a 20X-phase contrast objective, and digitized images were recorded periodically. Two images were obtained in Hepes-KSOM immediately prior to the introduction of hypoosmotic KSOM for the determination of initial diameter (at times designated t = -1.5 and -1.0 minutes). The solution exchange took approximately 1 minute ending at t = 0 minutes. Images were then obtained every 3 minutes, starting at t = 2 minutes. The last image was obtained at t = 29 minutes. The diameters of the zygotes were determined for each image using the line drawing function of the image analysis software (*isee* and *dsp/os*) to measure the distance between the same points on the circumference (plasma membrane) in successive images. The zygotes retained their spherical shape during swelling and subsequent recovery, as judged from the stored images.

For many experiments, including all those in which inhibitors were used and all those aimed at determining any role for intracellular Ca^{++}, the quantitation of the extent of

recovery from swelling was accomplished by calculating the percent recovery at 29 min. after the introduction of hypoosmotic KSOM. This time was chosen because control zygotes had, on average, just completed recovery from swelling. Thus, any treatment which abolished or slowed recovery would have an effect on the percent recovery at 29 min. If an earlier time point had been used, control recoveries would have been less than 100%; if a later time point had been used, some treatments which actually slowed recovery would have been missed.

Percent recovery was defined as $100x\ [(d_{max} - d_f) / (d_{max} - d_i)]$, where d_{max} was the maximum relative diameter reached, d_f was the relative diameter at 29 min, and d_i was the relative diameter at -1.5 min. Cell swelling was confirmed for each zygote by measuring the change in cell diameter over time. Percent recoveries for each treatment was reported as medians, with the data represented by box plots (see Figure 6). Those few embryos (2-3% of the total in all experiments) whose diameters did not increase by at least 8% (volume increase of 26%) were excluded from analysis, as they were judged to be osmotically unresponsive (Séguin and Baltz, 1997). The value of 8% was chosen because preliminary measurements showed a few zygotes, which swelled either not at all, or only a few percent, while the majority of zygotes swelled significantly. The value of 8% was empirically found to separate these populations.

Due to the desire to precisely quantitate the relative rate of recovery in

experiments measuring the inhibition of RVD in the presence of high concentrations of organic osmolytes, actual rates of recovery were calculated rather than percent recoveries at 29 min as described above. The rate of recovery was calculated from a linear least squares fit to the linear portion of recovery (i.e., the portion beginning when the zygote had maximally swelled), which yielded a slope describing the rate of change in diameter for each individual zygote as a function of time. This slope was then divided by the initial increase in diameter (difference between the maximum diameter and initial diameter) upon exposure to hypoosmotic KSOM medium, in order to normalize variability in swelling. This quantity was termed the relative recovery rate. As above, any zygotes, which did not increase in diameter by at least 8% upon hypoosmotic exposure, were excluded (1-2% of the total in all experiments). Where reported, times of 50% and 95% recoveries were calculated from the relative recovery rates.

Measurement of Intracellular Ca^{++} Concentration in Mouse Zygotes

The compounds used in these experiments were prepared as follows: Fura-2-AM (Molecular Probes Inc., Eugene, OR), BAPTA-AM (MPI), and 4-bromo-A23187 (MPI) were prepared as stocks in DMSO (dimethylsulfoxide; BDH, Toronto, ON). EGTA (Ethylene glycol-bis [ß-aminoethyl ether]-N,N,N',N'-tetraacetic acid) was added directly to the medium.

Intracellular Ca^{++} concentration was measured using the fluorescent Ca^{++} indicator fura-2. Fura-2 has strong fluorescent properties, minimal interference by cell autofluorescence and a greater selectivity for Ca^{++} over other divalents and heavy metals (Grynkiewicz et al., 1985; Tsien, 1980).

Fura-2-AM, a non-fluorescent esterified form of the indicator, was introduced into the zygote by incubation in the presence of pluronic acid (Sigma, St-Louis, MO), a carrier which makes the poorly soluble fura-2-AM indicator more soluble in water. The esterified indicator is uncharged and hydrophobic, and can readily cross the cell membrane. Once in the cytosol, endogenous esterases cleave the ester groups, releasing the free acid form of fura-2 which does not permeate the membrane and thus accumulates intracellularly. Zygotes were loaded with the fura-2-AM indicator by incubation with 2 μM of fura-2-AM for 30 minutes at 37°C. Fluorescence was recorded using 350 nm and 380 nm excitation wavelengths in rapid succession. At 350 nm, the Ca^{++}-bound form of the indicator fluoresces strongly, while at 380 nm the Ca^{++}-free form of the indicator is more fluorescent. Fluorescent images were gathered at an emission wavelength of 510 nm since this wavelength approximates fura-2's emission maximum. Images were recorded using an intensified charge-coupled device camera (DAGE CCD72, with Geniisys intensifier, DAGE-MIT, Michigan City, IN).

Ca^{++} concentration was determined in these experiments by ratiometric imaging using the ratio of the fluorescence intensity at 350 nm to that of 380 nm. This ratio is dependent on the concentration of Ca^{++}, but largely independent of other variables such as fluorophore concentration, cell thickness, etc. Conversion of this ratio to Ca^{++} concentration was accomplished by the method of Grynkiewicz, et al. (1985), employing the Ca^{++} ionophore 4-Br-A23187 (5 μM) in the presence of Ca^{++}, or EGTA (5 mM) in the absence of Ca^{++}. 4-Br-A23187 was used instead of A23187 because the latter fluoresces. In several experiments, the Ca^{++} chelator BAPTA was used to buffer intracellular Ca^{++} (loaded with BAPTA by incubation with 20 μM BAPTA-AM coincident with fura-2-AM incubation). For Ca^{++} measurement experiments, relative diameters were determined for each zygote using the square root of the area of each zygote's fluorescent image, which was determined automatically using the imaging system, rather than by direct measurement as in other experiments. These two methods yielded indistinguishable data for recoveries from swelling.

Permeability of Glycine

^{3}H-glycine (2-^{3}H-glycine, 2-5 μCi/mmol, Amersham, Arlington Heights, IL or New England Nuclear, Boston, MA) was added directly to the appropriate medium before each experiment.

^{3}H-glycine was used to measure the permeability of glycine in non-swelled and swelled mouse zygotes. Standard curves for each lot of ^{3}H-glycine were constructed from serial dilutions of ^{3}H-glycine spanning the range of counts measured in embryos. This allowed conversion of counts per minute to glycine concentration for each lot of ^{3}H-glycine. The determination of standard curves was repeated each week. The use of standard curves obtained under the same conditions used with zygotes (i.e., solutions, range of counts per minute due to ^{3}H) largely eliminated potential problems due to variations in counting efficiency and quenching, as these would be identical for the standard curves and experiments with zygotes.

To determine the ^{3}H-glycine content, zygotes were removed from the experimental medium, immediately washed several times in ice-cold Hepes-KSOM of the same osmolarity as the experimental medium, and transferred to scintillation vials. This was repeated for subsequent groups of zygotes until the complete experimental pool of zygotes had been transferred to scintillation vials. Four millilitres of scintillation fluid (Scintiverse BD; Fisher Scientific, Pittsburg, PA) were added to each vial to lyse the zygotes and the solutions were mixed. Mouse zygotes are very small (<100 μm diameter) and thus quenching even by unlysed zygotes would not be significant. However, it has been confirmed by direct observation under a dissecting microscope that zygotes were completely lysed within minutes of being placed in scintillation fluid (Dawson and Baltz,

unpublished). ^{3}H was detected using a 2200CA TriCarb liquid scintillation counter (Packard Instrument Co., Downer's Grove, IL). Each sample was counted for 5 minutes. Background samples were measured by taking medium from the last wash drop and the residual counts were determined. These counts were subtracted from the counts obtained for the zygote samples. Background was always a small fraction of the counts obtained in zygote-containing samples, indicating that the washing procedure was effective. The total glycine content of zygotes was calculated using the standard curves.

Glycine influx experiments consisted of incubating freshly-isolated zygotes in a 20-50 µl drop of Na^{+}-depleted hypotonic or isotonic medium, containing 2 µM ^{3}H-glycine at 37°C with 5% CO_2/air under oil. Na^{+}-depleted media were used to eliminate uptake by the glycine transport system found in zygotes, which is Na^{+}-dependent. After 15 minutes of incubation, groups of 20 zygotes were removed from the droplet and washed through four changes of ice-cold Hepes-KSOM medium without glycine. Influx rates were measured in hypotonic or isotonic media, and expressed as total accumulated glycine divided by 15 minutes to obtain the rate of glycine influx per minute. DIDS or ATP (500 µM and 5 mM respectively) were included in some hypoosmotic solutions, as indicated.

The few embryos (1-2% of the total in all experiments) that had lysed or ruptured when examined under the dissecting microscope at any stage of the experiments were discarded.

Data Analysis

Plots were generated using SigmaPlot for Windows 1.0 (Jandel Scientific, San Rafael, CA). Percent recovery data were plotted as box plots, which provide a visual depiction of the descriptive statistics (median, 10th, 25th, 75th, and 90th percentiles, outliers) of each population/treatment and were especially useful for the representations of zygote volume recoveries which were not normally distributed (Figure 6). To compare percent recoveries between treatment groups (control, Ca^{++}-dependence experiments, and nucleotide experiment), the nonparametric Kruskal-Wallis analysis of variance (ANOVA) test was employed, since preliminary investigations showed a significant inhomogeneity of the standard deviations by Bartlett's test (Instat, GraphPad Software) as well as significant deviation from a normal distribution. In cases where the initial test (Kruskal-Wallis ANOVA) indicated a significant difference between the medians, Dunn's multiple comparison test (Instat) was used to determine whether the differences between individual treatments were statistically significant.

Ca^{++} concentrations were reported as the mean ± the standard error of the mean (SEM). Comparisons were made between both groups using a Student's two tailed *t*-test (Excel, Microsoft, Redmond, WA) since the measurements within each BAPTA treatment were paired (i.e., before-and-after measurements on the same zygote). Before the *t*-test was applied, *F* tests were used to test whether the variances were homogenous,

and the appropriate *t*-tests assuming equal or unequal variances were then used as indicated.

Rates of RVD were reported as rates ± SEM. Relative recovery rates were compared after pooling the relative rates measured for each individual zygote within identical experiments, i.e., those with the same external compound present. Mean relative rates were computed for each compound and rates were compared using non-parametric ANOVA followed by Dunn's multiple comparison test (Instat).

^{3}H-glycine influx comparisons were performed using one-way ANOVA, followed by the Tukey-Kramer multiple comparison test. Influx was reported as mean accumulated amount of ^{3}H-glycine (fmol) per zygote/incubation time (15 min) ± SEM. Since, as described above, groups of embryos were pooled together and then divided into groups of 20 for counting, the values obtained for all of the sets of embryos from a single drop of medium were averaged after measurement.

Figure 6

Schematic diagram of a box plot representation

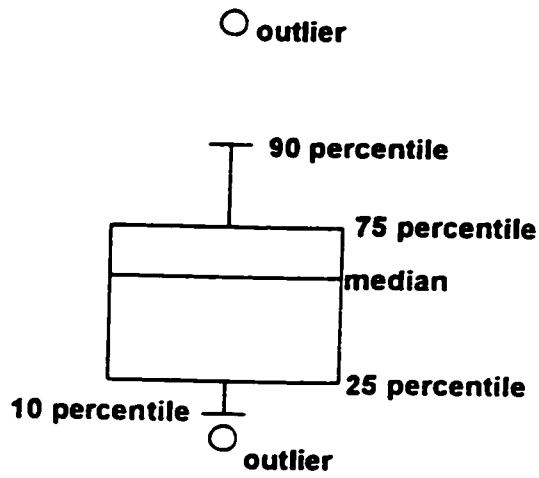
outlier
90 percentile
75 percentile
median
25 percentile
10 percentile
outlier

RESULTS

Intracellular Ca^{++} Measurements and Effect of Intracellular Ca^{++} Chelation

The initial experiments were aimed at determining whether intracellular Ca^{++} increased upon swelling in the mouse zygote. Intracellular Ca^{++} was therefore measured before and after hypotonic swelling by introduction of hypo-KSOM (0.63 x isotonic) within the same zygotes, using a protocol which was similar to that used to demonstrate RVD. An increase in Ca^{++} concentration was consistently observed when zygotes swelled (Figure 7A). Before swelling, the mean intracellular Ca^{++} concentration was 0.061 ± 0.002 μM ($n = 48$; $N = 5$). After the introduction of hypo-KSOM, at $t = 0$ minutes, Ca^{++} concentration increased to a mean of 0.120 ± 0.006 μM. This increase was highly significant ($P<0.001$ by *t*-test). Thus, intracellular Ca^{++} increased by approximately 0.06 μM when zygotes were hypotonically swelled.

Since intracellular Ca^{++} increased upon swelling, the effect of eliminating this Ca^{++} increase on the zygote's ability to perform RVD was examined. In several experiments, the Ca^{++} chelator BAPTA was used to buffer intracellular Ca^{++} and largely prevent any Ca^{++} increase. In zygotes that had been loaded with BAPTA, the mean Ca^{++} concentration before hypotonic exposure was 0.035 ± 0.002 μM ($n = 34$; $N = 3$). This was significantly lower than the 0.061 μM in zygotes in the absence of BAPTA ($P<0.001$), indicating that the presence of BAPTA resulted in a lower baseline Ca^{++}

concentration in zygotes. Upon hypotonic swelling, the intracellular Ca^{++} in BAPTA-loaded zygotes increased somewhat, to 0.057 ± 0.004 μM (Figure 7A); this increase was significant ($P<10^{-4}$). Nevertheless, the net increase in Ca^{++} was much smaller than in the absence of BAPTA, increasing by only 0.02 μM with BAPTA vs. 0.06 μM in control zygotes. Furthermore, the peak Ca^{++} concentration reached after hypotonic swelling in the presence of BAPTA (0.057 μM) was indistinguishable ($P>0.05$) from the Ca^{++} concentration in zygotes without the presence of BAPTA before induction of swelling (0.061 μM). Thus, the presence of BAPTA was able to greatly reduce the magnitude of the Ca^{++} increase, and to prevent the intracellular Ca^{++} concentration from rising above the baseline level in control zygotes.

The sizes of these same zygotes were concurrently measured during the intracellular Ca^{++} measurements using their fluorescent areas (as described in Materials and Methods). Zygotes loaded only with fura-2 were capable of performing RVD (Figure 7B). The median recovery at 29 minutes was 97% ($n = 28$; $N = 3$; in 2 of 5 fura experiments, the edges of the fluorescence images of zygotes due to lower loading of fura-2 were too indistinct for simultaneous size measurements). This recovery was not significantly different from the 113% recovery in the absence of fura-2 (control) as measured by direct measurement of the zygote diameter (Figure 7C; $P>0.05$ by Dunn's test). Thus, the presence of fura-2 in zygotes had no effect on RVD.

The presence of BAPTA in zygotes, which lowered baseline Ca^{++} concentration and greatly attenuated the Ca^{++} increase, had no effect on RVD (Figure 7B). At 29 minutes, median recovery in the presence of BAPTA was 91% (n = 33; N = 3), which was not significantly different from the 97% recovery in fura-2 loaded zygotes or the 113% recovery in the absence of fura-2 only (control) (Figure 7C; $P>0.05$ by Dunn's test). Thus, zygotes recovered from swelling identically in the presence or absence of BAPTA, indicating that the blunted Ca^{++} increase and low baseline Ca^{++} concentration in BAPTA-loaded zygotes did not affect their ability to recover from hypotonic swelling.

Effect of Ca^{++}-Dependent K^+ Channel Blockers

Clotrimazole, a compound which has been shown to be effective at blocking the Ca^{++}-dependent K^+ channel in erythrocytes (Brugnara et al., 1993), but which may also block other K^+ channels with lower affinity, showed a partial inhibition of mouse zygote RVD at 10 μM (Séguin and Baltz, 1997; Séguin, 1996). Since clotrimazole only demonstrated a partial inhibition on RVD in the zygote at a concentration of 10 μM, it was concluded that the type of Ca^{++}-dependent K^+ channel present in erythrocytes (a large conductance subtype) was not likely required for zygote RVD (Séguin and Baltz, 1997). The possibility remained, however, that another subtype of a Ca^{++}-dependent K^+ channel with different pharmacology could be mediating RVD. Thus, two other inhibitors

reported to inhibit Ca^{++} -dependent K^+ channels were tested. These experiments utilized charybdotoxin (100 nM) which blocks large-conductance Ca^{++} -dependent K^+ channels without effect on the small conductance subtype, and apamin (1 μM) which blocks small-conductance Ca^{++} -dependent K^+ channels without effect on the large conductance subtype (Burgess et al., 1981; Cook et al., 1983; Guggino et al., 1987; Maas et al., 1980; Moczydlowski et al., 1988; Talvenheimo et al., 1988; Tas et al., 1988; Weir and Weston, 1986).

Median recovery was 100% in the presence of charybdotoxin (n = 18; N = 2) and 112% in the presence of apamin (n = 20; N = 2) (Figure 7C). Therefore, neither charybdotoxin nor apamin had any significant effect relative to control ($P>0.05$ by Dunn's test). In contrast to what was previously shown with clotrimazole (a partial inhibition of RVD; $P>0.001$; Séguin, 1996), these more specific Ca^{++} -dependent K^+ channel blockers, charybdotoxin and apamin, did not inhibit RVD. Thus, volume recovery in mouse zygotes appears to be largely independent of Ca^{++} and not mediated by Ca^{++} -dependent K^+ channels which are inhibitable by either charybdotoxin or apamin (Figure 7).

Figure 7

Effects of Ca^{++} on mouse zygote RVD

A) Examples of intracellular Ca^{++} concentrations fura-2 loaded zygotes in the presence or absence of the Ca^{++} chelator BAPTA, during hypotonic swelling and recovery. Examples show the intracellular Ca^{++} concentration (μM) of a zygote over time (minutes).

B) Example of the relative diameters (μm) of fura-2 loaded murine zygotes undergoing RVD in the presence and absence of BAPTA. Zygotes recover their initial volume with a half time of about 10 minutes. Initial diameter measured in isotonic Hepes-KSOM at time -0.5 and -1 minute. Exposure to hypotonic bicarbonate-buffered KSOM at –1 minute.

C) Box plot representation indicating the distribution of percent recoveries (in terms of medians versus means) from the populations of zygotes exposed in a particular treatment. Box plots indicate the percentage of volume recovery of controls (n=14; N=3) and in the presence of fura-2 (n=28; N=3) and fura-2 and BAPTA (n=33; N=3) as well as in the presence of specific Ca^{++}-dependent K^+ channel blocker, charybdotoxin (n=18; N=2) and apamin (n=20; N=2). An open circle (outlier) represents one individual analysis which deviated from the population distribution (between the 10^{th} and 90^{th} percentiles. Significant differences between treatments and control are indicated with an asterix.

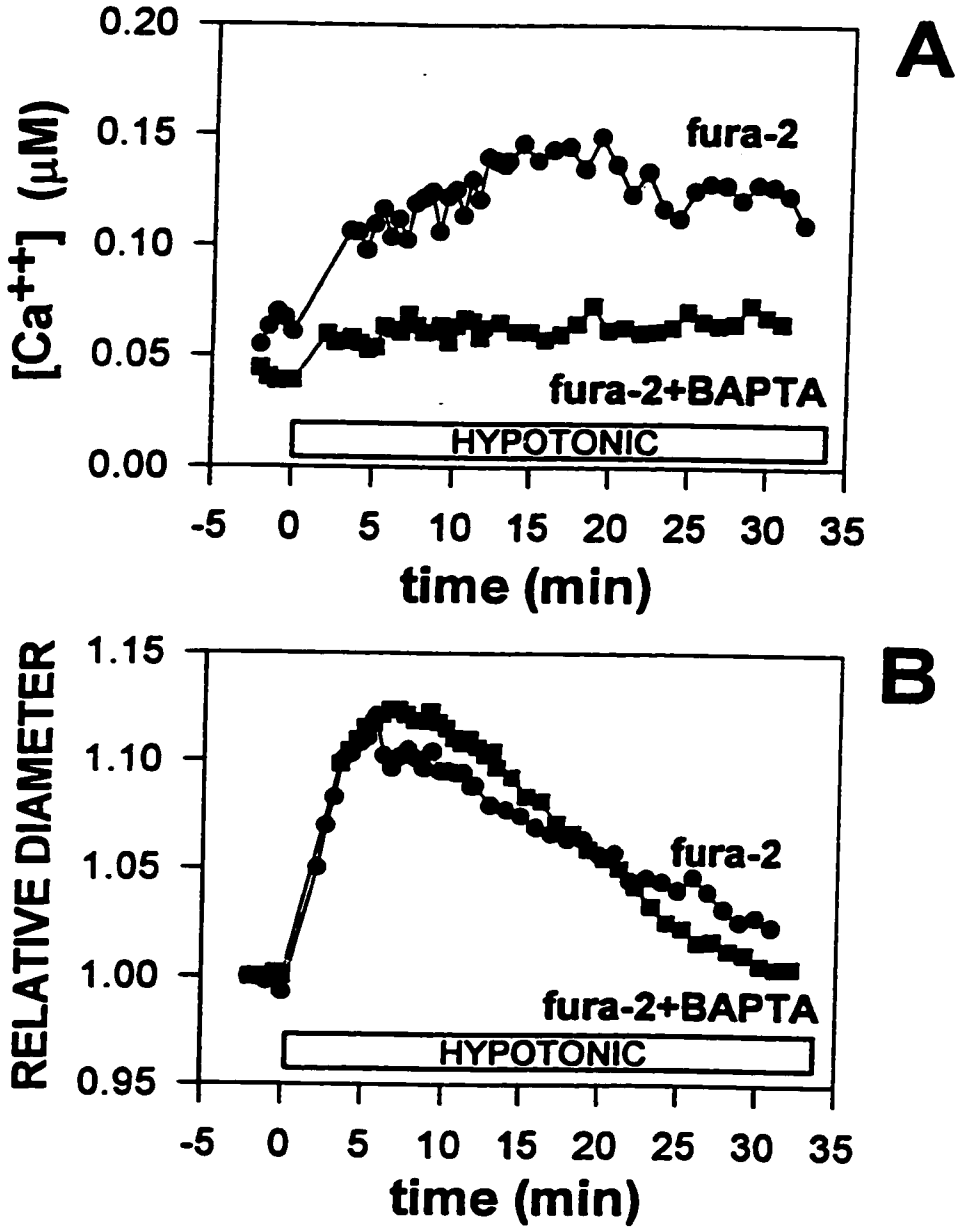
A
0.20
0.15
0.10
0.05
0.00
[Ca++] (μM)
fura-2
fura-2+BAPTA
HYPOTONIC
-5
0
5
10
15
20
25
30
35
time (min)
B
1.15
1.10
1.05
1.00
0.95
RELATIVE DIAMETER
fura-2
fura-2+BAPTA
HYPOTONIC
-5
0
5
10
15
20
25
30
35
time (min)

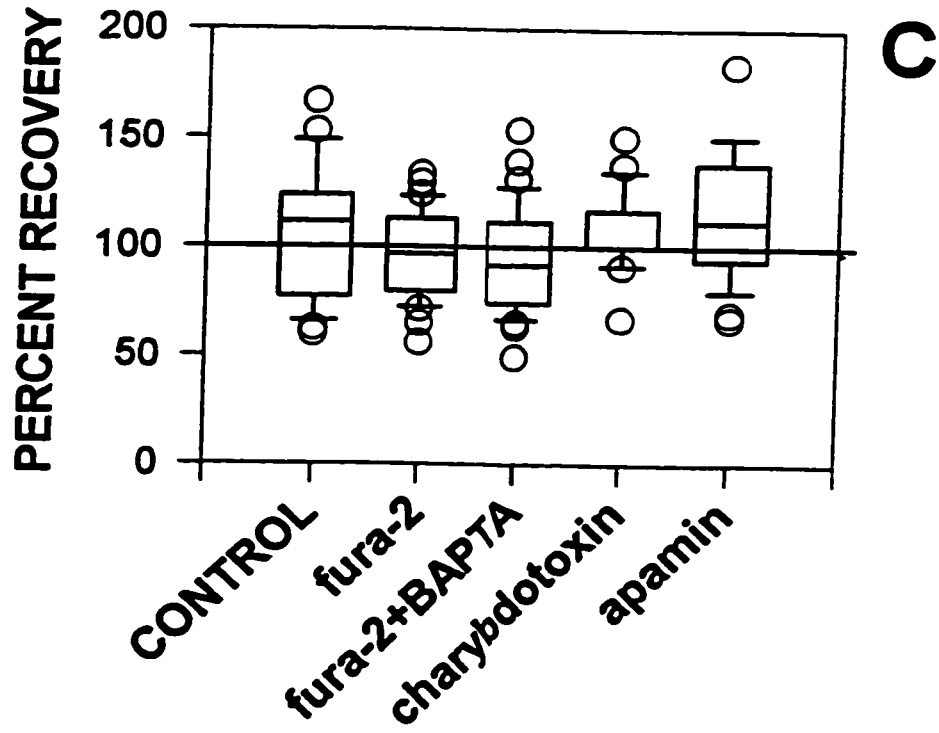
C
PERCENT RECOVERY
200
150
100
50
0
CONTROL
fura-2
fura-2+BAPTA
charybdotoxin
apamin

Effect of Extracellular Nucleotides

At millimolar levels, ATP has been reported to inhibit current carried by a volume-sensitive organic-osmolyte and anion channel in rat C6 glioma cells and other cells. This property is considered peculiar to the type of swelling-activated anion channel which is also permeable to organic osmolytes (VSOAC/VSOR channel; Jackson and Strange, 1995; Okada 1997; Strange et al., 1996). Because inhibition by external ATP at millimolar levels is considered diagnostic of the VSOAC/VSOR type of swelling-activated anion/organic osmolyte channel in other cell types, the effect of external ATP on RVD in zygotes was examined.

Mouse zygote RVD was completely inhibited by 5 mM ATP with a median recovery of 8% ($n = 37$; $N = 4$) at 29 min compared with 101% recovery for zygotes in control (Figure 8; $P<0.001$ by Dunn's test). This result indicated that it was possible that an ATP-inhibitable volume-sensitive anion and organic osmolyte channel functioned in mouse zygote RVD as it did in other cells. Consistent with this hypothesis was the finding that 0.1 mM ATP (i.e. submillimolar concentration) was without effect, since only millimolar levels of ATP were effective at blocking the VSOAC/VSOR channel in other cells. In mouse zygotes, median recovery in the presence of 0.1 mM ATP was found to be 100% ($n = 34$; $N = 4$) compared to 101% in control, which was not significantly different ($P>0.05$ by Dunn's test).

However, another possible mechanism for external nucleotide action is via purinoreceptors. P_2 type, but not P_1 type, purinergic receptors (Boarder et al., 1995; Brake et al., 1994; Kennedy and Leff, 1995; Stiles, 1992; Valera et al., 1994) would be activated by 0.1 mM ATP; however, as indicated above, this level of ATP had no effect on mouse zygote RVD. Thus, activation of P_2 purinergic receptors appeared not to be required for zygote RVD. Because 5 mM ATP would also activate the adenosine-specific P_1 receptor, adenosine was also tested for an effect on zygote RVD. In the presence of 5.0 mM adenosine, mouse zygotes still recovered from cell swelling. Median recovery for adenosine was 108% ($P>0.05$; $n = 16$; $N = 2$). Thus, P_1 purinergic receptors also appeared not to be involved in zygote RVD. The nucleotide, cAMP, was also tested since it is a related purine which had been described to inhibit swelling-activated Cl^- currents in Xenopus oocytes (Tsumura et al., 1996). In the presence of 5.0 mM cAMP, zygotes recovered, showing a median recovery of 108% ($P>0.05$; $n = 18$; $N = 2$), indicating that cAMP also had no effect on zygote RVD (Figure 8).

Figure 8

Effects of extracellular nucleotides on mouse zygote RVD

A) Examples showing the effects of extracellular nucleotides on zygote RVD. Examples show the relative diameter (μm) of a zygote over time (minutes) demonstrating the differences between control and in the presence of extracellular nucleotides ATP, adenosine and cAMP.

B) Box plot representation indicating the distribution of percent recoveries (in terms of medians versus means) from the populations of zygotes exposed in a particular treatment. Box plots indicate the percentage of volume recovery of controls (n=20; N=3) and in the presence of 5 mM ATP (n=37; N=4), 0.1 mM ATP (n=34; N=4), 5 mM adenosine (n=16; N=2) and 5 mM cAMP (n=18; N=2). An open circle (outlier) represents one individual analysis which deviated from the population distribution (between the 10^{th} and 90^{th} percentiles. Significant differences between treatments and control are indicated with an asterix ($P<0.001$ by Dunn's multiple comparison test).

A

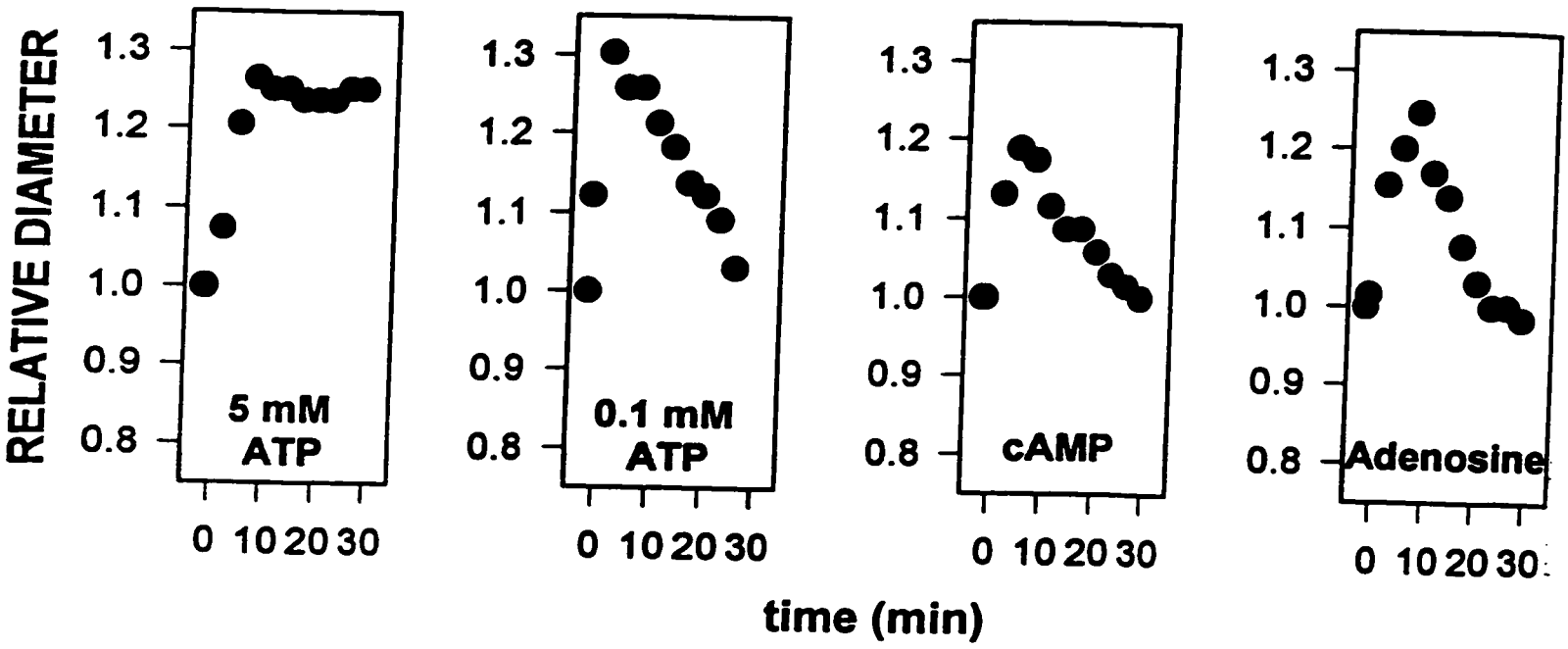
RELATIVE DIAMETER
1.3
1.2
1.1
1.0
0.9
0.8
5 mM ATP
0.1 mM ATP
cAMP
Adenosine
0 10 20 30
time (min)

B

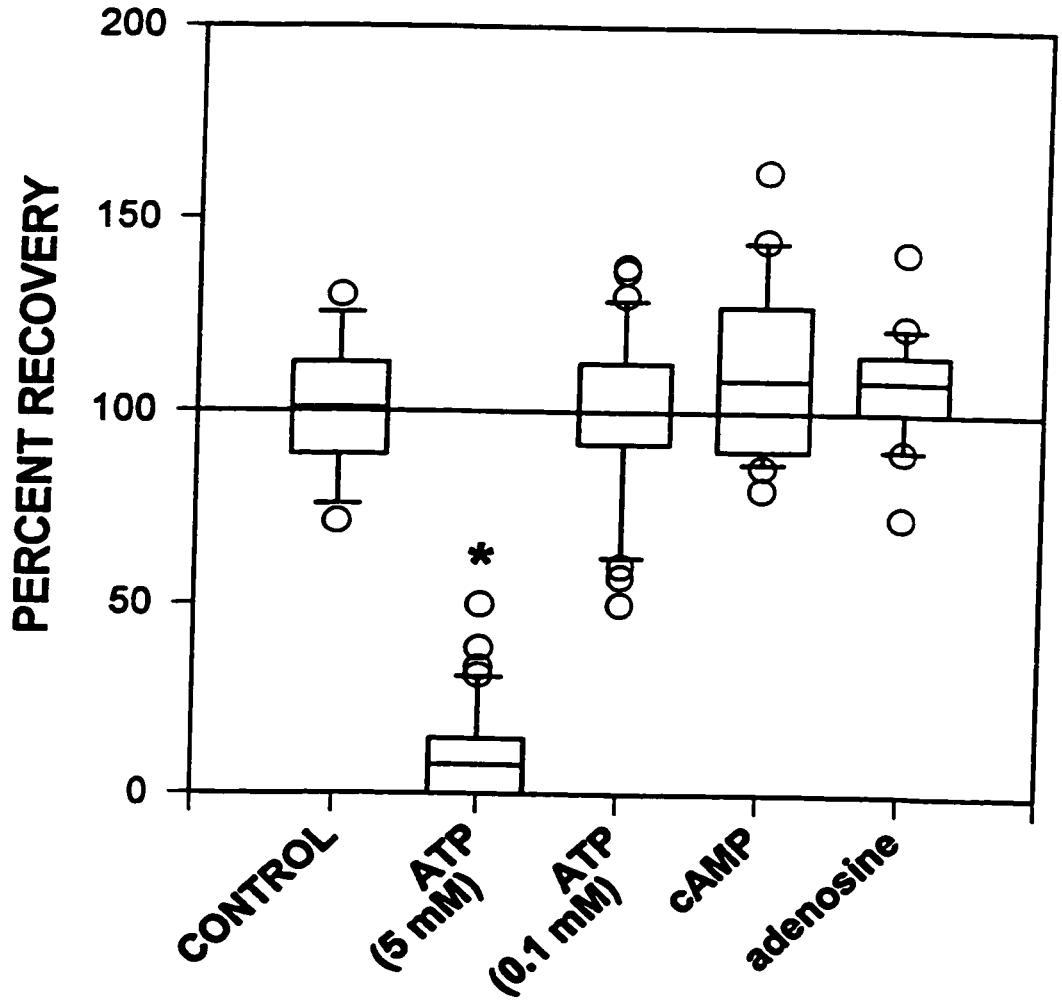
PERCENT RECOVERY
200
150
100
50
0
*
CONTROL
ATP (5 mM)
ATP (0.1 mM)
cAMP
adenosine

Effect of Large External Concentrations of Organic Osmolytes

To further characterize the swelling-activated organic osmolyte pathway in zygote RVD, a method was used which is similar to that developed by Passantes-Morales et al. (1993). This assay is designed to reveal which compounds can permeate the swelling-activated channel functioning in RVD. The method relies on the introduction of a large concentration of a compound to be tested into the external medium immediately after hypotonic swelling, when RVD would normally occur. When the channel opens upon cell swelling, normally intracellular osmolyte exit the cell, thus mediating RVD. However, if a large concentration of a compound which can permeate the swelling-activated pathway is present in the external medium, the imposed concentration gradient will cause a substantial influx ("backflux") of this compound into the cell upon swelling. This influx of an osmotically active substance will oppose RVD. Thus, permeability of a compound through the swelling-activated channel is revealed, in this assay, by its ability to block RVD. A number of compounds were tested. As a control, 50 mM of the trisaccharide raffinose was used, since it is an organic compound that cannot permeate nor be transported by mammalian cells.

RVD in the presence of raffinose was complete within 20 minutes after peak swelling, and was indistinguishable from RVD measured in zygotes in the absence of raffinose where NaCl provided the bulk of the osmotic support (Séguin and Baltz, 1997).

The mean rate of recovery in the presence of raffinose is shown in Figure 9.

Nineteen of the 20 common α-amino acids (tyrosine has too low a solubility and thus was excluded from these experiments) plus the β-amino acids taurine and β-alanine were tested using this assay for their effects on RVD. In addition, betaine, myo-inositol, and pyruvate were also assessed. Figure 9 shows the results, expressed as the mean rate of recovery from swelling in the presence of 50 mM of each of these compounds (except for aspartic acid and glutamic acid, where 25 mM of the Na^+ or K^+ salts were used to provide a similar osmolarity as 50 mM of the neutral compounds; see Discussion). The data have been sorted in Figure 9 so that those compounds with the greatest inhibition of RVD appear at the right.

Betaine and myo-inositol were included, because both are known to function as osmolytes in other cell types. Betaine, which has been shown to be osmoprotective in zygotes (Dawson and Baltz, 1997), was found to effectively oppose RVD, while myo-inositol, which has been shown to have no osmoprotective properties in zygotes (Dawson and Baltz, 1997) did not oppose RVD. Pyruvate was included because it is the preferred metabolic substrate in zygotes (Lawitts and Biggers, 1993) and it is known to permeate the swelling-activated anion/organic osmolyte channel in other cell types (Jackson et al., 1994).

Figure 9 shows that, generally, neutral and negatively-charged compounds

inhibited mouse zygote RVD, thus indicating that they are permeable when zygotes are swelled (Figure 9; $P<0.01$ by Dunn's test when compared to the control group which contained 50 mM raffinose). Positively charged compounds such as arginine, lysine, and histidine did not significantly inhibit RVD (Figure 9; $P>0.05$ compared to raffinose). Among the organic osmolytes tested, glycine was one of the most effective at inhibiting RVD (Figure 9).

Figure 9

Swelling-activated permeability of organic osmolytes

Data are represented as mean rate of recovery (min^{-1}) +/- SEM. Mean rate of recovery from swelling was examined instead of percent recovery for each treatment in order to correct for any effect of variable swelling. The data have been sorted so that those organic compounds with the greatest inhibition of RVD appear at the right. Each bar represents the mean and SEM of the rate of recovery in 2 to 4 replicates. The mean rate of recovery in the presence of raffinose represents the control group. Black bars represent the range of organic compounds which did not significantly inhibit RVD ($P>0.05$) when compared to raffinose. Grey bars indicate the range of organic osmolytes which did significantly inhibit RVD when compared to raffinose ($P<0.01$ by Dunn's test). White bars represent the range of organic compounds which did not significantly differ in their rate of recovery when compared to glycine and to raffinose ($P>0.05$).

Separate 'in graph' representation: Examples showing the relative change in diameter (μm) of a zygote over time (minutes) demonstrating the differences between control (RVD) and in the presence of extracellular glycine (no RVD).

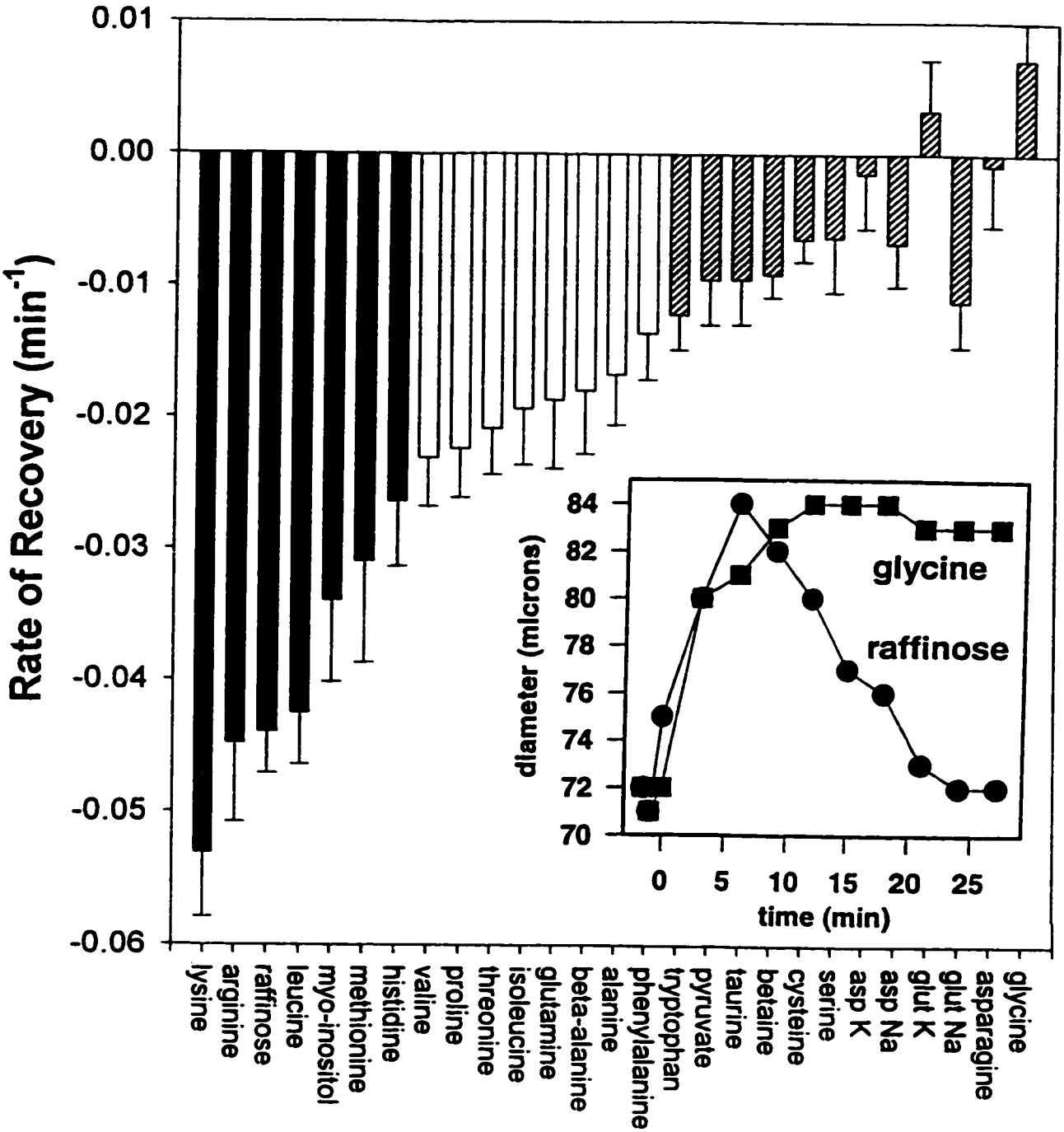
0.01
0.00
-0.01
-0.02
-0.03
-0.04
-0.05
-0.06
Rate of Recovery (min-1)
lysine
arginine
raffinose
leucine
myo-inositol
methionine
histidine
valine
proline
threonine
isoleucine
glutamine
beta-alanine
alanine
phenylalanine
tryptophan
pyruvate
taurine
betaine
cysteine
serine
asp K
asp Na
glut K
glut Na
asparagine
glycine
diameter (mlcrons)
84
82
80
78
76
74
72
70
0
5
10
15
20
25
time (min)
glycine
raffinose

^{3}H-glycine Influx

To directly test whether swelling increased the permeability of zygotes to organic osmolytes; the permeability of swelled zygotes to glycine was compared with the permeability of non-swelled zygotes using ^{3}H glycine. A Na^+-depleted medium was used to prevent interference by Na^+-dependent glycine uptake via the Na^+-dependent transporter Gly (Dawson et al., 1998). Zygotes were exposed to external ^{3}H glycine in either isotonic (non-swelled) or hypotonic (swelled) media. ^{3}H glycine (2 μM) was present beginning at the time the zygotes were transferred to hypotonic or isotonic media.

For these experiments, mouse zygotes were divided into four different groups. The first experimental group consisted of exposing freshly isolated zygotes to hypotonic medium in the absence of inhibitors (n = 180; N = 9). The second group was exposed to hypotonic medium in the presence of 500 μM DIDS (n = 100; N = 5). The third group was exposed to hypotonic medium in the presence of 5 mM ATP and (n = 120; N = 6) and the fourth group was exposed to isotonic medium in the absence of inhibitors (n = 100; N = 5).

Figure 10 indicates that glycine influx upon hypotonic exposure in the absence of inhibitors is significantly greater than in all other groups ($P<0.001$ by Tukey test). Glycine influx in hypo-KSOM in the presence of DIDS or ATP, and in isotonic medium was not significantly different from one another ($P>0.05$). Thus, from the data shown in

Figure 10, it appears that swelling induced an increased permeability to glycine in zygotes. This increase in permeability upon swelling was blocked by the presence of DIDS or ATP, which are known blockers of the swelling-activated Cl^- and organic osmolyte channel in the mouse zygote and other cells (Okada, 1997; Séguin and Baltz, 1997; Strange and Jackson, 1995). This inhibition is not due to an effect on the extent of swelling, as previous measurements had shown that neither DIDS nor ATP affected hypotonic swelling of zygotes (although both blocked RVD, above).

Figure 10

^{3}H-glycine influx in mouse zygotes

Data are represented as mean ^{3}H-glycine content (fmol) per zygote/incubation time (15 minutes) +/- SEM. Four different experimental approaches were used: hypo-KSOM (n=180; N=9), hypo-KSOM + DIDS (n=100; N=5), hypo-KSOM + ATP (n=120; N=6) and iso-KSOM (n=100; N=5). The inset shows the total amount of glycine accumulated after exposure to a particular treatment. The bars indicate the means +/- the SEM. Significant difference between treatments are indicated with an asterix ($P<0.001$ by Tukey-Kramer multiple comparison test).

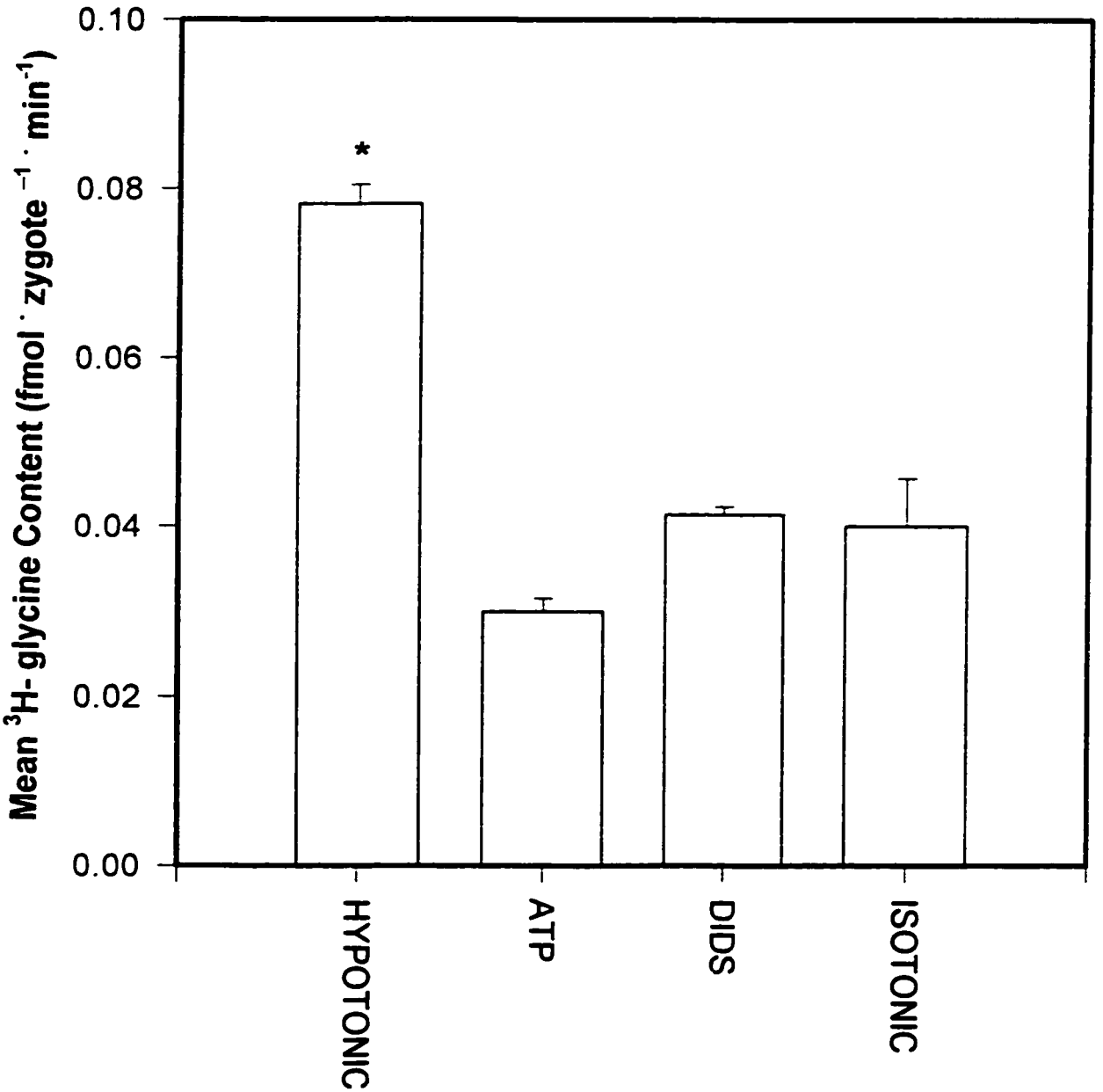
Mean ^{3}H- glycine Content (fmol · zygote $^{-1}$ · min $^{-1}$)
0.10
0.08
0.06
0.04
0.02
0.00
*
HYPOTONIC
ATP
DIDS
ISOTONIC

DISCUSSION

Mouse Zygote RVD

Mouse zygotes have been shown to recover from an imposed increase in volume, a process known as a regulatory volume decrease or RVD, recovering their initial volume after hypotonic exposure in less than 30 minutes (Results, and Séguin and Baltz, 1997). The inhibition of mouse zygote RVD by either blockers of Cl^- or K^+ channels initially indicated the participation of these channels (Séguin and Baltz, 1997). The rescue of RVD by gramicidin, a Na^+ and K^+ ionophore, in the presence of K^+ channel blockers but not Cl- channel blockers indicated that these were probably separate channels acting in concert, rather than a single molecular entity affected coincidentally by both types of channel blockers (Séguin and Baltz, 1997).

The presence of a swelling-activated Cl^- channel in mouse zygotes has since been directly demonstrated by electrophysiological measurements, confirming this model (Kolajova and Baltz, 1999). These whole cell patch clamp measurements directly supported many of the results reported here, which were obtained before the electrophysiological measurements were performed. First, a swelling-activated current was shown to exist, with current increasing by approximately 6-fold when zygotes were swelled. Second, the pharmacological characteristics of the swelling-activated current were consistent with those of RVD: the current was inhibited by DIDS (100 μM), NPPB

(10 μM), and external ATP (3 or 5 mM but not 1.0, 0.5, or 0.1 mM). Third, organic osmolytes such as taurine and aspartate were directly demonstrated to mediate swelling-activated current in zygotes, consistent with the high permeability of these compounds indicated in the present work.

The Involvement of Ca^{++} in Mouse Zygote RVD

Nothing was previously known about the signalling involved in activating the current upon zygote swelling. An increase in intracellular Ca^{++} has been shown to be required for RVD in some cell types, while RVD is independent of an increase in intracellular Ca^{++} in others (see above; Foskett, 1994). Thus, no *a priori* assumptions could be made about Ca^{++} signalling in mouse zygotes. A working hypothesis was that swelling induces an increase in intracellular Ca^{++} concentration in mouse zygotes, and that this increase is required for RVD. The first step in the investigation consisted of testing whether hypotonic swelling, under the same conditions that elicited RVD in zygotes (Séguin and Baltz, 1997), caused an increase in intracellular Ca^{++} concentration. The measurement of intracellular Ca^{++} during swelling was accomplished with the use of a ratiometric Ca^{++}-sensitive fluorophore, fura-2, which was loaded by incubation into the cytoplasm of the zygote. As shown in Figure 7, the apparent Ca^{++} concentration in mouse zygotes approximately doubled, at t = 3 minutes, upon cell swelling and remained

elevated throughout the experimental protocol. The change in fura-2 fluorescence ratio which occurred upon zygote swelling represented a change in intracellular Ca^{++} concentration, rather than being an artifact of the physical or optical changes which accompany swelling. This was confirmed by the ability of the Ca^{++} chelator, BAPTA, to greatly attenuate the change in fluorescence ratio, even though it had no effect on the extent of swelling. Since BAPTA does not fluoresce nor absorb in the relevant wavelengths for fura-2 measurements, the presence of BAPTA could only have affected intracellular Ca^{++} concentrations, but not other properties likely to produce artifacts. Therefore, it was concluded that an increase in intracellular Ca^{++} occurred upon hypotonic swelling in zygotes.

To determine if the observed increase in Ca^{++} was required for RVD, RVD was measured in the presence or absence of BAPTA. It was assumed that if the increase in Ca^{++} were required for RVD to occur, then RVD would be inhibited when BAPTA was present, since the chelator largely eliminated any increase in intracellular Ca^{++}. However, this increase in Ca^{++} did not appear to be required for RVD, since zygotes preloaded with the Ca^{++} chelator, BAPTA, recovered from swelling even though the Ca^{++} rise was severely blunted. Furthermore, the attenuated Ca^{++} increase failed to raise the level of Ca^{++} above the baseline (pre-swelling) concentration in the absence of BAPTA, indicating that an increase in Ca^{++} to a specific level was not required for RVD. These results are

consistent with those shown in Ehrlich ascites tumour cells and clonal N1E115 neuroblastoma cells (Foskett, 1994; Grinstein et al., 1982; Hoffman, 1985; Lippman et al., 1995; McCarty and O'Neil, 1992), where RVD has been shown to be independent of a global increase in Ca^{++}. These experiments do not rule out, however, the presence of localized increases in Ca^{++}, perhaps near the plasma membrane, which cannot be spatially resolved by the ratio imaging technique used. It is possible that BAPTA, while eliminating the global Ca^{++} increase, cannot attenuate such very localized increases.

Since one major function of Ca^{++} during RVD in some cells is to activate Ca^{++}-dependent K^+ channels, inhibitors of such channels were employed here to determine if such channels might participate in zygote RVD. It had previously been shown that clotrimazole, a K^+ channel blocker which has been found to completely block the charybdotoxin-sensitive, Ca^{++}-dependent K^+ channel in erythrocytes with an IC_{50} of well under 100 nM (Brugnara et al., 1993), was partially effective at blocking RVD in mouse zygotes when added at 10 μM (Séguin and Baltz, 1997). This finding is perhaps reflective of a low-affinity effect on another type of K^+ channel since the specificity of clotrimazole has not been determined for any K^+ channel types other than those in erythrocytes. It could also, however, indicate that a Ca^{++}-dependent K^+ channel mediates RVD in zygotes, but that its susceptibility to clotrimazole is different in zygotes than in erythrocytes. Therefore, the Ca^{++} -dependent K^+ channel blockers, apamin (1μM) and

charybdotoxin (100 nM) were tested to determine if zygote RVD was affected by these drugs. Apamin is a component of bee venom which specifically blocks the small conductance subtype (see above), whereas charybdotoxin is a component of scorpion venom which specifically blocks the large conductance subtype (see above). If either of these drugs blocked RVD in zygotes, then a role for Ca^{++}-dependent K^+ channels might be indicated.

As shown in figure 7, however, neither toxin demonstrated a significant effect on RVD, indicating that the particular Ca^{++}-activated K^+ channels, which are targets of these toxins, were not involved in zygote RVD. The formal possibility that these toxins are ineffective against these channels in zygotes, even though the channels are present cannot be ruled out, however.

Taken together, the data presented here indicated that it was unlikely that intracellular Ca^{++} served as a required signal for zygote RVD or that the large and small conductance subtypes of Ca^{++}-dependent K^+ channels were required for RVD in zygotes.

Swelling-Activated Permeability to Organic Osmolytes

Mouse zygotes have been shown to require organic osmolytes in order to maintain viability when cultured in medium with moderately increased osmolarity (Dawson and Baltz, 1997; Gardner and Lane, 1993; McKiernan et al., 1995; Van Winkle et al., 1994).

In addition, studies have shown that mouse zygotes accumulate glycine to provide intracellular osmotic support, and that zygotes can maintain a greater cell volume in media with moderately increased osmolarity (Dawson et al., 1998). All of this indicates that zygotes are capable of the regulated accumulation of organic osmolytes.

It would seem likely that zygotes must be able to release these accumulated organic osmolytes, as well as accumulate them. If they could not, then their ability to regulate intracellular osmolarity and cell volume would be incomplete. In many other cell types, this ability is conferred by a single type of swelling-activated anion channel (VSOAC/VSOR), which is permeable to inorganic anions, principally Cl^-, as well as to a range of organic osmolytes (see above; Okada, 1997; Strange et al., 1996). Hence, it was hypothesized that the swelling-activated Cl^- channel found in mouse zygotes would also be permeable to organic osmolytes. This type of channel has a characteristic set of pharmacological and functional properties which distinguish it from other known channels. One such distinguishing feature is a characteristic profile of pharmacological inhibitors. The swelling-activated anion/organic osmolyte channel in other cells is inhibitable by Cl^- channels blockers, as well as by external ATP in millimolar levels (Okada, 1997; Strange et al., 1996; Séguin and Baltz, 1997). It has been previously shown that common Cl^- channel blockers inhibited RVD in mouse zygotes (Séguin and Baltz, 1997; Séguin, 1996), indicating that a Cl^- channel was involved in mediating

mouse zygote RVD. Although some swelling-activated Cl^- channels (which are not permeable to organic compounds) are insensitive to stilbenes such as DIDS, RVD in mouse zygotes is completely blocked by DIDS (Séguin and Baltz, 1997; Séguin, 1996), indicating that such Cl^--specific channels are unlikely to be required for zygote RVD. Furthermore, mouse zygote RVD was inhibited by millimolar levels of external ATP (Figure 8), but not sub-millimolar levels: an inhibition profile considered diagnostic of the VSOAC/VSOR type of swelling-activated anion/organic osmolyte channel in other cells (e.g., C6 glioma cells; epithelial cells; Jackson and Strange 1995; Tsumura et al., 1996). Taken together, these findings indicated that a swelling-activated channel with pharmacological properties resembling those of the VSOAC/VSOR channel in other cells is required for RVD in mouse zygotes.

Extracellular cAMP did not affect mouse zygote RVD. cAMP has been reported to affect swelling-activated channels differently in different cell types. Xenopus oocytes have swelling-activated channels which are largely indistinguishable from the VSOAC channel in mammalian cells. This current is inhibited by external cAMP at millimolar levels as well as ATP (Ackerman et al., 1994). In contrast, however, cAMP does not inhibit the VSOAC channel in mammalian cells (e.g., epithelial cells; Tsumura et al., 1996). Therefore, the properties of mouse zygote RVD are consistent with those reported for the VSOAC/VSOR channel in other mammalian cells.

However, a possible alternative mechanism for external ATP action on RVD existed. This mechanism would be secondary signalling via purinoreceptors. Since 5 mM ATP is high enough to activate both the P_1 (highest affinity for adenosine) and P_2 (highest affinity for ATP) purinoreceptor subtypes, such a mechanism of action could not be ruled out. The strategy was to test 5 mM adenosine, which would completely activate the P_1 purinoreceptor, and to test a lower concentration of ATP that would be insufficient to block characterized VSOAC/VSOR channels, but would be sufficient to fully activate P_2 purinoreceptors.

To test whether P_1 type receptors might be implicated, 5 mM adenosine, which has been shown to fully activate P_1 class purinergic receptors (Boarder et al., 1995, Stiles, 1992) was used. Mouse zygote RVD was unaffected by the presence of 5 mM adenosine (Figure 8). Thus, inhibition of RVD secondary to activation of a P_1 type receptor by the very high levels of ATP used seems unlikely. Known P_2 class receptors, which have the highest affinity for ATP, are fully activated at 0.1 mM ATP (Brake et al., 1994; Kennedy and Leff, 1995; Valera et al., 1994). However, 0.1 mM ATP was found to have no discernible effect on RVD (Figure 8). This result makes it unlikely that P_2 type receptors were involved in ATP mediated inhibition of RVD. Therefore, the inhibition of RVD in the zygote by extracellular ATP does not appear to be mediated by any purinergic receptor pathways. However, given that only single doses were used throughout this

experimental protocol and that various receptor subtypes have been characterized (Table 1 and Table 2), it is not possible to completely rule out the presence of purinoreceptors with different affinities for adenosine and ATP than those previously characterized, whose activation might affect zygote RVD. Other known purinergic receptor blockers could be used to further test this possibility, but this would extend beyond the scope of this thesis.

Given these results, is appeared likely that a channel resembling the VSOAC/VSOR channel was present in mouse zygotes and mediating RVD. This channel would be predicted to serve as the pathway for swelling-activated release of organic osmolytes. Thus, it was expected that swelling would increase the permeability of zygotes to organic osmolytes, and that this permeability pathway would have similar pharmacological properties to RVD.

To characterize organic osmolyte permeability, a similar assay developed by Passantes-Morales et al., (1993) was used, which allowed the screening of a large number of compounds for increased permeability in swelled zygotes. This assay consisted of introducing a large concentration (50 mM for all compounds except for aspartic acid and glutamic acid at 25 mM) of each suspected osmolyte in the external medium during experimentally-induced hypotonic swelling. If the potential osmolyte were highly permeable, then RVD would be blocked due to a "backflux" of osmolyte through

swelling-activated pathway. As an osmolyte enters the cell, driven by the large imposed concentration gradient; it opposes the effect of any intracellular osmolytes which must be released upon cell swelling to allow RVD. Thus, this assay allowed the rapid screening of a large number of compounds for swelling-activated permeability, flagging their permeability through the swelling-activated anion channel.

The permeability to organic osmolytes of the hypotonically-activated pathway in mouse zygotes was examined by measuring the rate of RVD in the presence of each compound to be tested, as described above (Passantes-Morales et al., 1994; Passantes-Morales et al., 1993). Each compound's ability to inhibit RVD was assessed, and the compounds were arranged in Figure 9 according to their ability to inhibit RVD. Only a subset of all the compounds tested (those at the right) were found to be able to inhibit RVD.

Since the swelling-activated pathway which is permeable to osmolytes is proposed to function as an anion channel, it would be expected to have the highest permeability to those compounds with a net negative charge and to be impermeant to compounds which are positively charged (i.e., lysine, arginine, histidine; Figure 9). This was indeed the case. Lysine, arginine and histidine were unable to perturb RVD even when present at a 50 mM external concentration, while negatively charged amino acids such as aspartic acid and glutamic acid were extremely effective at blocking RVD. The

result with aspartic acid is especially significant, as it has been directly shown to be able to carry a swelling-activated current in zygotes (Kolajova and Baltz, 1999), supporting the validity of this assay in zygotes.

Furthermore, the effectiveness of a given compound in inhibiting RVD should be related, at least in part, to the average net charge on amino acids which are zwitterionic at physiological pH (Table 4). Thus, the more negatively charged amino acids should, on average, be more effective at blocking RVD than those with more net positive charge. Indeed, the ability to inhibit RVD was found to correlate with isoelectric point, with all compounds with isoelectric points below 6 being very effective at blocking RVD, and a decreasing effectiveness as isolectric point increased above pH 6 (Table 4).

Thus, the effectiveness of this assay in identifying compounds with significant permeability through the swelling-activated channels seems to be validated. First, those compounds which are known to be highly permeable to the swelling-activated VSOAC/VSOR channel in other cells (e.g., taurine, aspartic acid, glycine) were also identified as permeable by this assay. In addition, those compounds which have been shown to not permeate the swelling-activated pathway in other cells (e.g., lysine, arginine) were identified here as well. Furthermore, aspartate and taurine, which have been shown to exhibit a swelling-activated increase in current in mouse zygotes, and glycine, which was shown here to have a higher permeability in swelled zygotes than in

non-swelled zygotes, were all identified as permeable in this assay. Thus, this method has provided a survey of a large number of compounds, and identified those compounds which might, if present in the external medium, be appropriate to serve as organic osmolytes in mouse zygotes.

It is important to note that two of the compounds tested--aspartic acid and glutamic acid--were used at 25 mM external concentration while all of the others were used at 50 mM. This was due to their net negative charge at physiological pH, which requires a cation to accompany them. In order to have the same osmolarity in all solutions, only half the concentration of these two compounds could be used, with the other half of the osmotic balance being the accompanying Na^+ or K^+. This would appear to have had no effect on the assay. Both compounds completely inhibited RVD at 25 mM, with inhibitions not significantly different from the "best" compound, glycine. Thus, since inhibition was already not different from 100%, increasing their concentrations, even if possible would not increase the inhibition of RVD (which cannot significantly exceed 100%). Both Na^+ and K^+ were assessed as the accompanying cation, but, even though K^+ is more permeable to cells than Na^+, the two salts were equally effective. It might, however, be found that the K^+ salts are more effective at lower concentrations than the Na^+ salts, but this was not tested here, since the aim was to assess the ability of each compound tested to inhibit RVD at an essentially saturating

concentration. It should be noted that the K^+ salts demonstrated a larger inhibition in comparison to the Na^+ salts likely due to tonicity and because of the presence of a RVD dependent K^+ channel.

As an independent test for a swelling-activated permeability to organic osmolytes in zygotes, the organic compound glycine, which has been shown to have a role as an "osmolyte" in zygotes (Dawson et al., 1998; Dawson and Baltz, 1997), and which was identified in the experiments above (the "backflux" approach) as a highly-permeable compound, was used to directly demonstrate that permeability is directly increased upon cell swelling. This was done by examining whether the rate of influx of ^3H glycine was increased upon hypotonic swelling.

Glycine influx into swelled zygotes was found to be significantly higher than in non-swelled zygotes (Figure 10). It would stand to reason that an increase in glycine permeability upon swelling should have the same pharmacological properties as RVD if it were mediated by the same mechanism. This was confirmed using the stilbene DIDS and the nucleotide ATP, and showing that the swelling-activated increase in the influx of ^3H-glycine was abolished, and that it decreased to the level of influx seen in non-swelled zygotes in the absence of either inhibitor (Figure 10). This finding supports the earlier data of Van Winkle et al. (1994) that demonstrated that there was a swelling-activated increase in taurine permeability (in Na^+-free media like the media used here) which had

similar properties to the swelling-activated glycine influx. Thus, data obtained with a number of independent assays, including RVD measurements, patch clamp studies, and direct measurements of permeability, are consistent in identifying a set of organic compounds which can mediate RVD in zygotes, and which permeate the swelling-activated channel in zygotes that resembles the VSOAC/VSOR channel in other cells. These compounds include, notably, glycine, taurine, other amino acids, and betaine, which have been shown to be beneficial to in vitro embryo development and to act as organic osmolytes in preimplantation mouse embryos.

CONCLUSION

There are a number of different types of Cl^- and K^+ channels that have been shown to mediate RVD in various mammalian cell types. Studies have found that swelling-activated K^+ channels can be either Ca^{++}-activated or insensitive to Ca^{++} (Foskett, 1994) depending on the cell, while swelling-activated Cl^- channels can be either chloride-selective or permeable to a range of organic compounds (organic osmolytes) as well as inorganic anions (Okada, 1997; Strange and Jackson, 1995). Results presented here show that while the intracellular Ca^{++} concentration increased upon cell swelling in mouse zygotes, RVD nevertheless occurred normally in zygotes loaded with the Ca^{++} chelator, BAPTA, which prevented any increase of Ca^{++} above its normal resting level. In addition, inhibitors of known Ca^{++}-dependent K^+ channels, charybdotoxin and apamin, had no effect on RVD. This indicates that Ca^{++} signalling or Ca^{++}-activated K^+ channels are probably not required for RVD in the mouse zygote.

Mouse zygote RVD was inhibited by 5 mM extracellular ATP. Millimolar concentrations of ATP had previously been shown to block the current carried by the swelling-activated anion channel, which is also permeable to organic osmolytes, in other cells (Jackson and Strange, 1995; Okada, 1997, Strange and Jackson, 1995). Thus, the inhibition of mouse zygote RVD by extracellular ATP is an indication that a swelling-activated Cl^- channel with similar properties could be present in mouse zygotes

and participate in RVD. Mouse zygote RVD was also insensitive to millimolar levels of cAMP, again consistent with the properties of the swelling-activated Cl^- channel in other mammalian cells. Inhibition of RVD in mouse zygotes secondary to activation of any purinergic receptors was deemed unlikely since submillimolar levels of ATP and millimolar levels of adenosine were ineffective. Hence, consistent with the data presented here, it is proposed that the Cl^- and organic osmolyte channel in mouse zygotes is indeed a swelling-activated Cl^-/organic osmolyte channel like that found in many other cells and termed the VSOAC/VSOR channel. In fact, recent electrophysiological studies performed by Kolajova and Baltz (1999) have directly revealed the presence of a swelling-activated Cl^- channel with properties identical to the VSOAC/VSOR channel in mouse zygotes, consistent with the findings presented here and with this proposal.

REFERENCES

Ackerman, MJ, KD Wickman, and DE Clapham. Hypotonicity activates a native chloride current in Xenopus oocytes. J. Gen. Physiol. 103:153-179, 1994.

Anbari, K, and RM Schultz. Effect of sodium and betaine in culture media on development and relative rates of protein synthesis in preimplantation mouse embryos in vitro. Molec. Reprod. And Devel. 35: 24-28, 1993.

Banderali U, and G Roy. Anion channels for amino acids in MDCK cells. Am. J. Physiol: The Cell 32:C1200-1207, 1992.

Biggers, JD, JA Lawitts, and CP Lechene. The protective action of betaine on the deleterious effects of NaCl on preimplantation mouse embryos in vitro. Molec. Reprod. Devel. 34:380-390, 1993.

Boarder, MR, GA Weisman, JT Turner, and GF Wilkinson. G protein-coupled P_2 purinoreceptors: from molecular biology to functional responses. TIPS 16:133-139, 1995.

Borland, RM, S Hazra, JD Biggers, and CP Lechene. The elemental composition of the

environments of gametes and preimplantation embryo during the initiation of pregnancy. Biol. Reprod. 16:147-157, 1977.

Botchkin LM, and G Matthews. Swelling activates chloride current and increases internal calcium in nonpigmental epithelial cells from the rabbit ciliary body. J. Cell Physiol. 164:286-294 (1995).

Brake, AJ, MJ Wagenbach, and D Julius. New structural motif for ligand-gated ion channels defined by an ionotropic ATP receptor. Nature 371:519-523, 1994.

Brugnara, C, L de Franceschi, and SL Alper. Inhibition of Ca^{++}-dependent K^{+} transport and cell dehydration in sickle erythrocytes by clotrimazole and other imidazole derivatives. J. Clinical Invest. 92:520-526, 1993.

Burgess, GM, M Claret, DH Jenkinson. Effects of quinine and apamin on the calcium-dependent potassium permeability of mammalian hepatocytes and red cells. J. Physiol. 317: 67-90, 1981.

Burnstock, G, and C Kennedy. Is there a basis for distinguishing two types of P_2

purinoreceptors? Gen. Pharmacol. 16:433-440, 1985.

Burnstock, G. A basis for distinguishing two types of purinergic receptor. In: *Cell membrane receptors for drugs and hormones* (ed. L Bolis and RW Straub) Raven Press, New York. pp. 107-118, 1978.

Cala, PM. Cell volume regulation by Amphiuma red blood cells: the role of Ca^{++} as a modulator of alkali metal/H^{+} exchange. J. Gen. Physiol. 82: 761-784, 1983.

Carmines, PK. Segment-specific effect of chloride channel blocker on rat renal arteriolar contractile responses to angiotensin II. A. J. Hypertension. 8:90-94, 1995.

Castle, NA, DG Haylett, DH Jenkinson. Toxins in the characterization of potassium channels. Trends Neuros. 12: 59-65, 1989.

Chamberlin, ME, and K Strange. Anisosmotic cell volume regulation; a comparative view. Am. J. Physiol: The Cell 26:C159-C172, 1989.

Chatot, CL, CA Ziomek, BD Bavister, JL Lewis, and I Torres. An improved culture

medium supports development of random-bred 1-cell mouse embryos in vitro. J. Reprod. Fert. 86:679-688, 1989.

Collins, JL and JM Baltz. Estimates of mouse oviductal fluid tonicity based on osmotic responses of embryos. Biol. Reprod. 60:1188-1193, 1999.

Cook, NS, DG Haylett, PN Strong. High affinity binding of [^{125}I]monoiodoapamin to isolated guinea-pig hepatocytes. FEBS Lett. 152: 265-269, 1983.

Dalziel, HH, and DP Westfall. Receptors for adenine nucleotides and nucleosides; subclassification, distribution, and molecular characterization. Pharmacol. Reviews 46:4:449-466, 1994.

Davidson, A, M Vermesh, RA Lobo, and RJ Paulson. The temporal effects of changes in in vitro fertilization culture media on the one-cell mouse embryo system. J. in Vitro Fert. And Embryo Transfer 5:3:149-152, 1988.

Dawson, KM, JL Collins and JM Baltz. Osmolarity-dependent glycine accumulation indicates a role for glycine as an organic osmolyte in early preimplantation mouse

embryos. Biol. Reprod 59: 225-323, 1998.

Dawson, KM, and JM Baltz. Organic osmolytes end embryos: substrates of the Gly and β transport systems protect mouse zygotes against the effects of raised osmolarity. Biol. Reprod 56:1550-1558, 1997.

Duan, D, JR Hume, S Natrel. Evidence that outwardly-rectifying chloride channels underlie volume -regulated chloride currents in heart. Circ. Res. 80:103-113, 1997.

Duan, D, C Winter, S Cowley, JR Hume, and B Horowitz. Molecular identification of a volume-regulated chloride channel. Nature. 390:417-421, 1997.

Duan, D, B Fermini, and S Natrel. Alpha-adrenergic control of volume-regulated Cl^- currents in rabbit atrial myocytes. Circ. Res. 77:379-393, 1995.

Erbach, GT, JA Lawitts, VE Papaioannou, and JD Biggers JD. Differential growth of the mouse preimplantation embryo in chemically defined media. Biol. Reprod. 50:1027-1033, 1994.

Fatherazi, S, KT Izutsu, RB Wellner, CM Belton. Hypotonicity activated chloride current in HSG cells. J. Membr. Biol. 142:181-193, 1994.

Foskett, JK. The role of calcium in the control of volume-regulatory transport pathways. In: *Cellular and Molecular Physiology of Cell Volume Regulation* (ed. K Strange) CRC Press, Boca Raton, FL. pp. 259-277, 1994.

Fredholm, BB, MP Abbracchio, G Burnstock, JW Daly, TK Harden, KA Jacobson, P Leff, and M Williams. Nomenclature and classification of purinoreceptors. Pharmacol. Reviews 46:2:143-156, 1994.

Gallin, EK, TM Mason, and A Moran. Characterization of regulatory volume decrease in the THP-1 and HL-60 human myelocytic cell lines. J. Cell Physiol. 159: 573-581, 1994.

Garcia-Perez, A, MB Burg. Role of organic osmolytes in adaptation of renal cells to high osmolarity. J. Membr. Biol. 119: 1-13, 1991.

Gardner, DK, and M Lane. Amino acids and ammonium regulate mouse embryo development in culture. Biol. Reprod. 48:377-385, 1993.

Geck, P, B Pfeiffer. $Na^+ + K^+ + 2\ Cl^-$ cotransport in animals cells-its role in volume regulation. Ann. NY Acad. Sci. 456: 166-182, 1986.

Grinstein, SA, JD Goetz-Smith, D Stewart, BJ Beresford, A Mellors. Protein phosphorylation during activation of Na^+/H^+ exchange by phorbol esters and by osmotic shrinking: possible relation to cell pH and volume regulation. J. Biol. Chem. 261: 8009-8016, 1986.

Grinstein, SA, A Dupre, A Rothstein. Volume regulation by human lymphocytes: role of calcium. J. Gen. Physiol. 79: 849-868, 1982.

Grynkiewicz, G, M Poenie, and RY Tsien. A new generation of Ca^{++} indicators with greatly improved fluorescence properties. J. Biol. Chem. 260:3440-3450, 1985.

Guggino, SE, WB Guggino, N Green, B Sacktor. Blocking agents of Ca^{++}-activated K^+ channels in cultures medullary chick ascending limb cells. Am. J. Physiol. 525:C128-C137, 1987.

Hallows, KR, and PA Knauf. Principles of cell volume regulation (Ch.1), In: *Cellular*

and Molecular Physiology of Cell Volume Regulation (ed. K Strange) CRC Press, Boca Raton, FL. pp. 3-29, 1994.

Hay-Schmidt, A. The influence of osmolality on mouse two-cell development. J. Assist. Reprod. Genet. 10:95-98, 1993.

Hoffman, EK, and LO Simonsen. Membrane mechanisms in volume and pH regulation in vertebrate cells. Physiol. Rev. 63:315, 1989.

Hoffman, EK. Role of separate K^+ and Cl^- channels and of Na^+/Cl^- cotransport in volume regulation in Ehrlich cells. Federation Proc. 44: 2513-2519, 1985.

Jackson, PS, and K Strange. Characterization of the voltage-dependent properties of a volume-sensitive anion conductance. J. Gen. Physiol. 105:661-677, 1995.

Jackson, P., R Morrison, K Strange. The volume-sensitive organic osmolyte channel VSOAC is regulated by nonhydrolytic ATP binding. Am. J. Physiol. 267, 36: C1203-C1209, 1994.

Jennings, ML and RK Schultz. Okadaic acid inhibition of KCl cotransport: evidence that protein dephosphorylation is necessary for activation of transport by either cell swelling or N-ethylmaleimide. J. Gen. Physiol. 97: 799-818, 1991.

Kaji, DM, and Y Tsukitani. Role of protein phosphatase in activation of KCl cotransport in human erythrocytes. Am. J. Physiol. 260: C176-C182, 1991.

Kenakin, TP, RA Bond, and TI Bonner. Definition of pharmacological receptors. Pharmacol. Reviews 44:351-361, 1992.

Kennedy, C, and P Leff. How should P_{2x} purinoreceptors be classified pharmacologically? TIPS 16:168-174, 1995.

Kirk, K, JC Ellory, and JD Young. Transport of organic substrates via a volume-activated channel. J. Biol. Chem. 267:33:23475-23478, 1992.

Kolajova, M and JM Baltz. Volume-regulated anion and organic osmolytes channels in mouse zygotes. Biol. Reprod., 60:964-972, 1999.

Kolb, HA. Potassium channels in excitable and non-excitable cells. Physiol. Biochem. Pharmacol. 115: 51-91, 1990.

Kwon, HM, and JS Handler. Cell volume regulated transporters of compatible osmolytes. Curr. Opin. Cell Biol 7:465-471, 1995.

Law, RO. Amino acids as volume-regulatory osmolytes in mammalian cells. Comp. Biochem. Physiol. A Comp. Physiol. 99: 263-277, 1991.

Lawitts, JA, and JD Biggers. Culture of preimplantation embryos (Ch.9), In: *Guide to Techniques in Mouse Development, Methods in Enzymology* v.255 (ed. PM Wasserman and ML DePamphilis) Academic Press, San Diego, CA. pp. 153-164, 1993.

Lawitts, JA, and JD Biggers. Overcoming the 2-cell block by modifying standard components in a mouse embryo culture medium. Biol. Reprod. 45: 245-251, 1991.

Lee, SC, and C Deutsch. Temperature dependence of K^+-channel properties in human T lymphocytes. Biophys. J. 57: 49-62, 1990.

Levinson, C. Volume regulatory activity of the Ehrlich ascites tumour cells. Biochim. Biophys. Acta 1021: 1-8, 1990.

Lippmann, BJ, R Yang, DW Barnett, and S Misler. Pharmacology of volume regulation following hypotonicity-induced cell swelling in clonal N1E115 neuroblastoma cells. Brain Res. 686:29-36, 1995.

Lopes, AG, and WB Guggino. Volume regulation in the early proximal tubule of the Necterus kidney. J. Membr. Biol. 97: 117-125, 1987.

Maas, AJ, J Den Hertog, A Ras, J Van Den Akker. The action of apamin on guinea-pig taenia caeci. Eur. J. Pharmac. 67: 265-274, 1980.

MacLeod, RJ, P Lembessis, JR Hamilton. Effect of osmotic swelling on K^+ conductance in jejunal crypt epithelial cells. Am. J. Physiol. 262:G1021-G1026, 1992.

Martini, FH, WC Ober, CW Garrison, K Welch, and RT Hutchings. *Fundamentals of Anatomy and Physiology.* (ed. DK Brake) Prentice Hall Inc. Upper Saddle River, NJ. 1998.

McCarthy, NA, and RG O'Neil. Calcium signalling in cell volume regulation. Physiol. Reviews 72:4:1037-1061, 1992.

McKiernan, SH, MK Clayton, and B Bavister. Analysis of stimulatory and inhibitory amino acids for development of hamster one-cell embryos in vitro. Molec. Reprod. and Devel. 42:188-199, 1995.

Miyoshi, K, H Funahashi, K Okuda, and K Niwa. Development of rat one-cell embryos in a chemically defined medium: effects of glucose, phosphate and osmolarity. J. Repro. Fert. 100:21-26, 1994.

Moczydlowski, E, K Lucchesi, A Ravindran. An emerging pharmacological of peptide toxins targeted against potassium channels. Membr. Biol. 105: 95-111, 1988.

Neufield, T, D. Terreros, J Grantham. Critical role of calcium in the regulation of intracellular volume of isolated proximal S2 renal tubules in hypotonic medium. Kidney Int. 23:225, 1983.

Oda, K, WE Gibbons, and SP Leibo. Osmotic shock of fertilized mouse ova. J. Reprod.

Fert. 95:737-747, 1992.

Okada, Y. Volume expansion-sensing outward-rectifier Cl^- channel: fresh start to the molecular identity and volume sensor. Am. J. Physiol: the Cell 42:C755-C798, 1997.

Passantes-Morales, H, RA Murray, R Sanchez-Olea, and J Moran. Regulatory volume decrease in cultured astrocytes II. Permeability pathway to amino acids and polyols. Am. J. Physiol: the Cell 35:C172-C178, 1994.

Passantes-Morales, H, S Alvalez, R Sanchez-Olea, and J Moran. Contribution of organic and inorganic osmolytes to volume regulation in rat brain cells in culture. Neurochem. Res. 18:445-452, 1993.

Phillips, KP and JM Baltz. Intracellular pH change does not accompany egg activation in the mouse. Molec. Reprod. Devel. 45:52-60, 1996.

Pusch, M, and TJ Jentsch. Molecular physiology of voltage-gated chloride channels. Physiol. Rev. 74: 813-827, 1994.

Sadler, TW. *Langman's Medical Embryology* (ed. Bill Cady) Williams and Wilkins, Baltimore, MD, 1995.

Sakardi, B, and JC Parker. Activation of ion transport pathways by changes in cell volume. Biochim. Biophys. Acta 1071: 407-427, 1991.

Schauf, C, D Moffett, and S Moffett. *Human Physiology*. (ed. D Allen) CV Mosby Company, St-Louis, MO. 1990.

Schumacher, PA, G Sakellaropoulos, DJ Phipps, LC Schlichter. Small-conductance chloride channels in human peripheral T lymphocytes. J. Membr. Biol. 145: 217-232, 1995.

Séguin, DG, and JM Baltz. Cell volume regulation by the mouse zygote: mechanism of recovery from a volume increase. Am. J. of Physiol: the Cell 41:C1854-C1861, 1997.

Séguin, DG. Cell volume regulation by murine zygotes. Honours Thesis, Department of Physiology (submitted), 1996

Seki, G, S Taniguchi, S Uwatoko, K Suzuki, K Kurokawa. Activation of the basolateral Cl^- conductance by cAMP in rabbit renal proximal tubule S3 segments. Pflugers Arch-Eur. J. Physiol. 430: 88-95, 1995.

Spindle, A. Beneficial effects of taurine on mouse zygotes developing in protein-free culture medium. Theriogenology. 44: 761-772, 1995.

Stiles, GL, Adenosine Receptors. J. Biol. Chem. 267:6451-6454, 1992.

Strange, K, F Emma, and PS Jackson. Cellular and molecular physiology of volume-sensitive anion channels. Am. J. Physiol. 270:C711-C730, 1996.

Strange, K, and PS Jackson. Swelling-activated organic osmolyte efflux: a new role for anion channels. Kidney Int. 48:994-1003, 1995.

Sukudi, M, K Kawahara, A Ogawa, T Morita, Y Kawaguchi, S Kurihara, O Saki. $[Ca^{++}]_i$ rises via G protein regulatory volume decrease in rabbit proximal tubule cells. Am. J. Physiol. 258: F690-F696, 1990.

Talvenheimo, JA, G Lam, C Gelband. CTX inhibits the 250 pS Ca^{++}-activated K^+-channel in aorta and contracts aorta smooth muscle. Biophys. J. 53:258a, 1988.

Tas, PWL, HG Kress, K Koschel. Presence of charybdotoxin-sensitive Ca^{++}-dependent K^+ channel in rat glioma C6 cells. Neuros. Lett. 94: 279-284, 1988.

Thiemann, AS, M Grunder, M Pusch, TJ Jentsch. A chloride channel widely expressed in epithelial and non-epithelial cells. Nature Lond. 356: 57-60, 1992.

Tsien, RY. Biochemistry 19: 2396-2404, 1980.

Tsumura, T, S Oiki, S Ueda, M Okuma, and Y Okada. Sensitivity of volume-sensitive Cl^- conductance in human epithelial cells to extracellular nucleotides. APStracts: 3:0232C, 1996.

Ueda, Y, and RH Steinberg. Chloride currents in freshly isolated rat retinal pigment epithelial cells. Exp. Eye Res. 58: 331-342, 1994.

Valera, S, N Hussy, RJ Evans, N Adami, RA North, A Suprenant, and G Buell. A new

class of ligand-gated ion channels defined by P_{2x} receptor for ATP. Nature 371:516-519, 1994.

Van Renterghem, C, P Vigne, C Frelin. A charybdotoxin-sensitive, Ca^{++}-activated K^{+} channel with inward rectifying properties in brain microvascular endothelial cells: properties and activation by endothelins. J. Neurochem. 65: 1274-1281, 1995.

Van Winkle, LJ, M Patel, HG Wasserlauf, HR Dickinson, and AL Campione. Osmotic regulation of taurine transport via system ß and novel processes in mouse preimplantation conceptuses. Biochim. Biophys. Acta 1191:244-255, 1994.

Van Winkle, LJ, D Hachighat, and AL Campione. Glycine protects preimplantation mouse conceptuses from a detrimental effect on development of the inorganic ions in oviductal fluid. J. Exp. Zool. 253:215-219, 1990.

Yamaguchi, DT, J Green, C Kleeman, S Muallem. Characterization of volume-sensitive, calcium-permeating pathways in the osteosarcoma cell line UMR-106-01. J. Biol. Chem. 264: 4383-4390, 1989.

Yancey, PH. Compatible and counteracting solutes. In: *Cellular and Molecular Physiology of Cell Volume Regulation* (ed. K Strange) CRC Press , Boca Raton, FL. p. 81-109, 1994.

Yancey, PH, ME Clark, SC Hand, RD Bowlus, and GN Somero. Living with water stress: evolution of osmolyte systems. Science 217:1214-1222, 1982.

Weir, SS and AH Weston. Effect of apamin on responses to BRL 34915, nicorandil and other relaxants in the guinea pig taenia caeci. Br. J. Pharmac. 88: 113-120, 1986.

Weiss, H, and F Lang. Ion channels activated by swelling of Madin-Darby canine kidney (MDCK) cells. J. Membr. Biol. 126: 109-114, 1992.

Zhao, Y, P J-P Chauvet P, SL Alper, and JM Baltz. Expression and function of bicarbonate/chloride exchangers in the preimplantation mouse embryo. J. Biol. Chem. 270: 24428-24434, 1995.

APPENDICES

Other Reagents

Organic Compounds: L-glycine, L-glutamine, L-glutamic acid (monosodium salt), L-glutamic acid (monopotassium salt), L-aspartic acid (monohydrate, sodium salt), L-aspartic acid (hemihydrate, potassium salt), L-proline, L-alanine, L-serine, L-cysteine, L-asparagine (monohydrate), L-arginine, L-leucine, L-isoleucine, L-lysine (monohydrochloride), L-valine, L-phenylalanine, L-tryptophan, L-methionine, L-threonine, L-histidine, ß-alanine (3-Aminopropionic), L-taurine, betaine (monohydrate), L-myo-Inositol (meso-Inositol; i-Inositol), pyruvic acid (sodium salt), were all, except arginine, directly added to the medium. Arginine, on the other hand, because of its basic pH was firstly dissolved in millipore water (Millipore: filtering unit which filters water several times to ensure low impurities), and pH adjusted by the addition of concentrated HCl, to make a 1000 x stock before its use.

Table 3

Physiological Properties of Organic Osmolyte Experimentation

Substrates	Number of Embryos/Number of Replicates	Osmolarity of Media (mOsm)	pH of Media*
Raffinose (control)	20/4	154	7.45-7.52
Leucine	14/3	162	7.37-7.47
Isoleucine	18/3	154	7.48-7.51
Lysine	14/3	185	7.38-7.50
Valine	19/4	188	7.46-7.53
Phenylalanine	18/4	177	7.37-7.49
Tryptophan	17/2	151	7.45-7.57
Methionine	15/3	171	7.47-7.57
Histidine	19/2	152	7.51-7.59
Threonine	19/3	159	7.53-7.60
Glycine	21/3	152	7.47-7.58
Glutamine	17/4	160	7.41-7.52
Glutamate (sodium)	16/3	154	7.48-7.56
Glutamate (potassium)	18/2	183	7.45-7.50
Aspartate (sodium)	17/3	155	7.47-7.55
Aspartate (potassium)	15/2	156	7.44-7.5
Proline	16/4	161	7.43-7.51
L-alanine	20/3	154	7.46-7.53
Serine	21/3	165	7.43-7.51
Cysteine	18/3	183	7.48-7.57
Asparagine	18/3	152	7.35-7.48
Arginine	15/3	170	7.37-7.47
Taurine	17/3	158	7.38-7.51
Betaine	16/3	154	7.41-7.52
Myo-inositol	15/4	185	7.55-7.63
Puruvate	18/3	175	7.49-7.61
β-alanine	18/3	166	7.46-7.60

* Fluctuations in pH are due to the bicarbonate buffer in medium which changes when in atmosphere

Table 4

Physiochemical Properties of Biologically Important L-Amino Acids

Adapted from Yancey (1994)

Solute	Solubility (mmol/l)	Enthalpy (kcal/mol)	log K_d		Isoelectric Point	Partition Coefficient[101]
			Ca^{2+}	Mg^{2+}		
Alanine	1.867	387	1.2	2.0	6.00	520
β-Alanine	6,117				6.89[15]	
Arginine	861	894	2.2	1.3	10.76	
Asparagine	226	461			5.41	
Aspartate	38	383	1.6	2.4	2.77	
Betaine	13.396					
Cysteine	395		<4		5.07	
Cystine	<1	725			5.06[102]	
Glutamate	58	537	1.4	1.9	3.22	
Glutamine	291	614			5.65	
Glycine	3.329	231	1.4	1.3	5.97	991
Histidine	268				7.59	330
Isoleucine	314	856			6.02	48.5
Leucine	185	856			5.98	33.0
Lysine					9.74	
Methionine	665				5.74	74.5
Phenylalanine	179	1,111			5.48	22.5
Proline	14,101				6.30	
Sarcosine	4,804					
Serine	2,379	348	1.4		5.68	
Taurine	837		1.6[103]		5.16[15]	
Threonine	491				5.60	
Tryptophan	56	1,345			5.89	
Tyrosine	2	1,062	1.5	2.0	5.66	
Valine	756	698			5.96	